



OpenAIR@RGU

The Open Access Institutional Repository at Robert Gordon University

<http://openair.rgu.ac.uk>

Citation Details

Citation for the version of the work held in 'OpenAIR@RGU':

MOHAMMED, A. O., 2007. Evaluation and testing of a novel photocatalytic reactor with model water pollutants. Available from *OpenAIR@RGU*. [online]. Available from: <http://openair.rgu.ac.uk>

Copyright

Items in 'OpenAIR@RGU', Robert Gordon University Open Access Institutional Repository, are protected by copyright and intellectual property law. If you believe that any material held in 'OpenAIR@RGU' infringes copyright, please contact openair-help@rgu.ac.uk with details. The item will be removed from the repository while the claim is investigated.



CENTRE FOR RESEARCH IN ENERGY AND THE ENVIRONMENT (CRE+E)

SCHOOL OF ENGINEERING

FACULTY OF SCIENCE AND TECHNOLOGY

EVALUATION AND TESTING OF A NOVEL PHOTOCATALYTIC REACTOR

WITH MODEL WATER POLLUTANTS

MOHAMMED ABDULRAHMAN OLAWOLE

B.Eng, MSc. (Chem. Eng.)

This thesis is submitted in partial fulfilment of the requirements for the degree of Master of Research in Environmental Engineering at the Robert Gordon, University, Aberdeen.

May, 2007

RESEARCH DEGREES SELF-DECLARATION (RDDECL) FORM



RESEARCH DEGREES COMMITTEE

Research Student's Declaration Form

Name: MOHAMMED ABDULRAHMAN OLAWOLE

Degree for which thesis is submitted: MSC (Research)

Thesis title: EVALUATION AND TESTING OF A NOVEL
PHOTOCATALYTIC REACTOR WITH MODEL ORGANIC
POLLUTANTS

1 Material submitted for award

- (a) I declare that I am the sole author of this thesis.
- (b) I declare that all verbatim extracts contained in the thesis have been identified as such and sources of information specifically acknowledged.
- (c) I certify that where necessary I have obtained permission from the owners of third party copyrighted material to include this material in my thesis.
- (d) *either* *I declare that no material contained in the thesis has been used in any other submission for an academic award.

- (e) I agree that a copy of the thesis be held in The Robert Gordon University Library Electronic Thesis repository with full public access, that a paper copy (if available) be held in The Robert Gordon University Library, and that The Robert Gordon University supplies the British Library with a copy of the thesis in paper or electronic format for further distribution and inclusion in a central electronic repository with full public access, with the following status:

*Release the entire thesis immediately for access worldwide

I retain the ownership rights to the copyright of my work. I retain the right to use all or part of this thesis in future works (such as books and articles).

I hereby grant to The Robert Gordon University the non-exclusive right to archive and make accessible my thesis, in whole or in part in all forms of media. I agree that for purposes of preservation file format migration may be carried out should this be necessary.

2 Concurrent registration for two or more academic awards

I declare that while registered as a research student for the Robert Gordon University's research degree, I have not been a registered research student or enrolled student for another award of the University or other academic or professional institution.

Signature of Research Student Date

Signature of Principal Supervisor Date

This section of the form is for internal use only, for completion by the Convener of the Research Degrees Committee

Approved	
Rejected	
Reason for decision	
Signed	
Date	

ABSTRACT

Semiconductor photocatalysis is a newly emerging technology for the elimination of harmful chemical compounds from air and water. It couples low-energy ultraviolet light with semiconductors acting as photocatalyst and thereby overcoming many of the drawbacks that exist for the traditional water treatment methods. Recent literature has established the potential of this powerful technology to destroy toxic pollutants dissolved or dispersed in water. However, to date, very few viable pilot plants exist using this technology.

In this study, the application of photocatalysis for the removal of contaminants from waste water discharges such as produced water from oil rigs and other organic contaminants in industrial wastewater, were investigated. A novel photocatalytic reactor, which employs a commercial pellet titanium dioxide (TiO_2) catalyst, was tested for water treatment capability by investigating the photocatalytic degradation of contaminants from waste water discharges such as; hydrocarbons in produced water from the oil industry and synthetic dyes from the textile industry's waste processing fluids, using titanium dioxide (TiO_2) as photocatalyst in an aqueous suspension under UV irradiation.

Experiments were conducted to investigate the effects of parameters such as catalyst loading, pollutant adsorption rate on the pellet TiO_2 catalyst and reactor circulation flow rate. In this work, the batch adsorption of methylene blue from aqueous solution ($10\mu\text{M}$) onto the Hombikat-KCO pellet TiO_2 catalyst was studied, adsorption isotherms and kinetics were determined from the experimental data. A modest catalyst loading of 30g per 1L TiO_2 was chosen for further experiments since it shows gradual and consistent degradation results and approximately 98% degradation of methylene blue was achieved within 60 minutes irradiation in the optimization experiment.

Photodegradation of methylene blue dye was monitored by UV- spectroscopy. Complete degradation of methylene blue was achieved within 60 minutes illumination with the various loads of catalyst (30-200g). Experimental results indicate that this novel reactor

configuration has a high effective mass transfer rate and UV light penetration characteristics. The use of TiO₂ Hombikat KOC pellets catalyst means the system is free from the need of filtration of catalyst following photocatalysis and provides a higher surface area for catalyst illumination and a high contact of catalyst surface area with contaminated water.

ACKNOWLEDGEMENT

My profound gratitude goes to almighty Allah for His infinite mercy and protection throughout the duration of the study.

I would like to show deep appreciation to my supervisors, Dr. Cathy McCullagh and Prof. Pat. Pollard for their unrelenting support and invaluable guidance throughout the research work. They have made my time here both productive and enjoyable. I could not have had better supervision and consider myself lucky to have to work with them.

I would also like to extend thanks to Prof. Peter Robertson and Dr. Stephine Rigby for the supervision of the initial stages of the study.

Special thanks go to Morgan Adams, Simon Officer, and Pradbhu Radhakrishna for many intriguing discussion and consultations during the research. I also thank Dorothy McDonald and Martin Simpson for the administrative assistance on the research.

My gratitude goes out to my friends and family; Fatima, Hakeem, Abd Ganiyu, Zik Ibraheem, Yekini Abudu, Seun Elias, Ping Guo, and many others who have made my life outside work very enlightening.

TABLE OF CONTENTS

CONTENTS	PAGE
Title page	i
Declaration	ii-iii
Abstract	iv-v
Acknowledgement	vi
Table of Contents	vii-viii
List of Tables	ix
List of Figures and Illustrations	x
CHAPTER I INTRODUCTION	1-3
1.1 Chemical and Physical Treatment Processes	3-5
1.2 Research Overview	5
1.3 Aim and Objective of Study	5-7
CHAPTER II LITERATURE REVIEW	
2.1 Heterogeneous Photocatalysis	8
2.2 Reaction Mechanisms of TiO ₂ photocatalysis	9-11
2.3 Photocatalytic Reactor Technologies	11-20
CHAPTER III METHODS AND MATERIALS	
3.1 Reactor Set-up	21-23
3.2 Materials	24
3.3 Methods	
3.3.1 Batch Degradation Experiment	24
3.3.2 Continuous Flow Experiment	24
3.3.2.1 Dark Adsorption	24-25
3.3.2.2 Control Experiment	25
3.3.2.3 Degradation Experiment	25
3.3.3 Analytical Methods	

3.3.3.1	Calibration Plots	25-27
3.3.3.2	Total Organic Carbon (TOC) Analysis	27-28
CHAPTER IV RESULTS AND DISCUSSION		
4.0	System Optimization	29
4.1	Adsorption Equilibrium	29-31
4.2	Adsorption Isotherm	31-33
4.3	Batch Degradation Experiment	33-39
4.4	Methylene Blue TOC Analysis	39
4.5	Continuous Flow Degradation	40
4.5.1	Effect of Number of reaction Vessel	40-44
4.5.2	Effect of Recirculation rate	45-46
4.5.3	Congo Red dye (CR) Degradation	46-48
4.5.4	Acridine Orange (AO) Degradation	48-49
4.5.5	Produced Water Mineralization	50-52
4.6	Methylene Blue Batch Degradation with P-25 TiO ₂	52-54
CHAPTER V CONCLUSIONS AND FUTURE WORK		55-57
CHAPTER VI REFERENCES		58-66
CHAPTER VII APPENDIX		67-76

LIST OF TABLES

Table	Page
2.1 Oxidation Power of various species relative to Chlorine	10
3.0 Summary kinetics data of MB batch Degradation on TiO ₂	36
4.0 Methylene blue continuous flow reaction rate constants	38
5.0 Methylene blue reaction rate constants (effect of recirculation rate)	46
6.0 Water Chemistry analysis of oilfield produced water	51

LIST OF FIGURES

Figures	Page
3.1 Emission spectra of UV lamps	21
3.2 Schematic of the photoreactor configuration	22
3.3 Methylene Blue Absorption spectra	26
3.4 Methylene Blue calibration Plot	26
4.1 Adsorption of MB on TiO ₂ pellet	30
4.2 Freundlich Plot of methylene Blue Adsorption	33
4.3 Methylene Blue Batch degradation plot	34
4.4 First-order-reaction kinetics of MB degradation on 60 g/L	36
4.5 Rate of Change in Methylene Blue degradation with 30g TiO ₂	38
4.6 First-order-reaction kinetics of methylene blue degradation on 30g TiO ₂	38
4.7 Depletion in TOC of methylene blue mineralization	39
4.8 Continuous flow MB Adsorption	40
4.9 Continuous flow methylene blue degradation (1-vessel)	41
4.10 Continuous flow degradation of methylene blue (2-vessels)	42
4.11 Continuous flow degradation of methylene blue (3-vessels)	42
4.12 Continuous Flow methylene blue degradation with 1, 2, &3 Vessels	43
4.13 Comparison batch vs. continuous flow	44
4.14 Effect of Recirculation rate	45
4.15 Congo red continuous flow photocatalytic degradation	47
4.15 Congo red Dye mineralization	48
4.16 Acridine Orange photocatalytic degradation	49
4.17 Acridine Orange mineralization	49
4.18 Sample produced water Mineralization	50
4.19 First-order reaction kinetics of produced water demineralization	44
4.20 Change in methylene blue degradation P-25	53
4.21 First-order-reaction kinetics of methylene blue degradation on P-25 TiO ₂	53

CHAPTER 1

INTRODUCTION

1.0 Introduction

The efficient treatment of industrial wastewater and contaminated drinking water sources has become of immediate importance in a world that is faced with ever increasing population and decreasing energy resources [1]. An ideal wastewater treatment process will completely mineralize all the toxic species present in the waste stream without leaving behind any hazardous residues; it should also be cost effective. At the current state of development, none of the treatment technologies approaches this ideal situation [2, 3].

Pollution of ground water and rivers by organic pollutants is a constant concern and a common problem throughout the world. Many of these organic pollutants are; herbicides, pesticides, and fungicides used in agricultural activities, which can be carried away by rain and polluted water resources [4], hydrocarbons from wastewater discharges from oil production activities [5] and synthetic dyes from textile industry's waste processing fluids [6].

The oil and gas industry produces a wide variety of waste streams from its operations. The largest of which is produced water; with an estimated 670 million tonnes generated worldwide [7]. Studies on the impacts of produced water on the environment indicated that although not as acute as a large oil spill, the cumulative effects of the continued discharge of an even small amount of hydrocarbons does have a significant impact on the marine environment [8, 9].

There are a broad range of environmental issues relating to the effect of hydrocarbon presence on marine life, and on the aesthetic and commercial values of an impacted site. These issues include; the effect of direct exposure to oil in water on fish, marine mammals, and birds; the effect of oil on bottom-dwelling and inter-tidal species and the effect on commercial and or recreational resources and facility. The organic component of produced water has the potential to be degraded by aerobic microbes, the activities of which may reduce the dissolved oxygen levels in the ambient water

[5, 10] as well as releasing nutrients like nitrates and phosphates; this will drastically affect the aquatic life of the receiving water.

The reduction in the oxygen concentration in water brought about by the activities of the aerobic microbes and is compensated for by diffusion of oxygen from the water surface and from surrounding areas of higher oxygen concentration. This replenishment process is however slow, and as the oxygen level drops, anaerobic microbes, which can oxidize organic compounds without the presence of oxygen, start to thrive. The end products from the activities of these microbes are hydrogen sulphide, methane and ammonia [11]. These products are toxic to higher organisms.

When the temperature of water is increased, there will be a decrease in the waste assimilation capacity of the water; by depletion of dissolved oxygen and aerobic bacteria. This results in the destruction of algae and other plankton, thereby destroying fish food supply. Under continuous outfall of heavy organic pollution, the effect on water quality and oxygen levels is such as to impose a clear downstream zonation of animal, plant and microbial population [11].

Textile dyes and other commercial colourants have become the focus of environmental remediation efforts because their natural biodegradability is made increasingly difficult owing to the improved properties of dyestuffs [12]. A total of 15% of the total world production of dyes is lost during the dyeing process and is released in textile effluents [13, 14]. The release of this coloured wastewater in the ecosystem is a significant source of aesthetic pollution, of eutrophication and of perturbation in the aquatic life [13]. Colour interferes with penetration of sunlight into the water, retards photosynthesis, inhibits the growth of aquatic biota and interferes with solubility in water bodies [15].

At present, the most commonly employed method of removing pollutants present in industrial wastewater are the primary and secondary treatment methods, and sometimes the tertiary treatment methods, which involves the use of the various physical techniques (including phase transfer), thermal, chemical and biological processes to remove commonly found organics and inorganic contaminants. In most cases it is usually a combination of the primary and the secondary treatment methods

[16]. The primary processes are basically pre-treatment processes normally used to prepare the wastewater for secondary processes, which in most cases is biological treatment. The techniques used in the primary process are either physical or chemical (or combination of both) separation process to remove the coarse fraction, oil, fatty acids and suspended solids.

1.1 Chemical and Physical treatment Processes

Conventional chemical (coagulation, precipitation/neutralization) and physical (activated carbon adsorption, sedimentation, hydrocyclone, floatation cell, and air stripping) treatment techniques currently and commonly practiced technology for the removal of organic contaminants in industrial wastewaters are inherently problematic in their application. Chemical treatment methods can prove costly to the user as the active agent cannot be recovered for reuse in successive treatment cycles [17]. Also, the end-product is usually a large amount of sludge requiring final disposal.

Air stripping [16], which is commonly employed for the removal of volatile organic contaminants in water, just transfers the pollutants from the water phase to an air phase rather than destroy them. Thus, most air-stripping processes currently used require subsequent treatment of the off-gas. Similarly, hydrocyclone and flotation cell equipment currently employed for dispersed oil separation from oil industry's wastewater [18, 19] merely removed as much oil from the water and concentrate it for subsequent suction to storage facilities for final disposal.

Granular activated carbon (GAC) adsorption is the other commercial process for water purification. However, the spent carbon, on which pollutants are adsorbed, is a new waste that required disposal [2]. Biological degradation of municipal waste has been practiced, but similar bio-treatment of industrial waste is still not common because some toxic organic may kill the active micro-organism [2]. Although processes based on aqueous-phase hydroxyl radical chemistry are powerful oxidation methods to destroy toxic organic compounds they either use high-energy ultraviolet light or strong oxidants that are hazardous and are undesirable [16]. Some other chemical treatment processes may be directly destructive in nature, such as direct photolysis, using strong oxidants like $\text{H}_2\text{O}_2/\text{UV}$, O_3/UV and $\text{H}_2\text{O}_2/\text{O}_3/\text{UV}$. However,

the selection of operating parameters is very much dependent on the type of pollutants present [9, 20]. In addition, several intermediates, sometimes of more hazardous nature than the parent compounds, are formed in these processes and because of very low efficiencies, overall treatment costs become high if destruction of intermediates and complete mineralization need to be achieved [21].

However, many of the dyes used for industrial processes were insufficiently removed by conventional sewage plant treatment because of their high biochemical stability, their relatively high molecular weight, and high water solubility relative to their excellent all-round fastness [22].

As international environmental standards are becoming more stringent, (ISO 14001, 1996), a technological system for the removal of organic pollutants, such as dyes has to be developed. Heterogeneous photocatalysis is one of the advanced oxidation process (AOP) that has proven to be a promising method for the elimination of toxic and bio-resistant organic and inorganic compounds in wastewater by transforming them into innocuous species [8, 23, 24]. This process exploits the high oxidation potential of hydroxyl radicals that are produced by the illumination of a semiconductor photocatalyst with photons in the near ultraviolet spectrum [25].

AOPs not only oxidized the organic compounds, complete mineralization is achievable, the processes are not specific and therefore are capable of destroying a broad range of organic compounds [26]. The process is very powerful, and is immune to organic toxicity [27]. AOPs not only disinfect the water from virulent microbes, but can also remove toxic heavy metals [28], organic pesticides and solvents, chlorinated compounds, and inorganic chemicals from water without producing a waste stream unsuitable for disposal or consumption. For example, these processes can be used for chemical spill clean up, treatment of industrial effluents, and wastewater treatment [25].

In AOP, the hydroxyl radicals (OH^\bullet) can be produced by several pathways, including reactions such as; Fenton($Fe(II)/H_2O_2$) and photo-fenton catalytic reactions, H_2O_2/UV , O_3/UV , O_3/H_2O_2 , UV/H_2O and TiO_2 mediated photocatalysis.

Among the AOPs, heterogeneous photocatalysis using TiO_2 as photocatalyst has been shown to be one of the most effective destructive technology [51]. Its key advantages includes: its inherent destructive nature; non poisonous and it is relatively inexpensive, unlike other AOPs like the photolytic induced oxidation with ozone or hydrogen peroxide which will result in expensive high energy requirement if the organic or inorganic pollutants of waste water strongly absorb UV-radiation. The utilization of metal salt Fe (II) as Fenton's reagent produces inorganic sludge that may cause a waste disposal problem [25, 29].

1.2 Research Overview

The main focus in reducing the possible aquatic pollution from hydrocarbon discharge to the sea has traditionally been on reducing the content of dispersed oil. Even though some countries have placed their attention on other compounds, international regulations like the new OSPAR regulations still focus mainly on dispersed oil content in produced water [7]. The new OSPAR regulation demands less than 30 mg/l dispersed oil, and a 15% reduction in total oil from year 2000 level, with implementation in year 2006 and the industry's goal of zero discharge [7] gives impetus to the development of new techniques for the removal of dispersed oil in the produced water.

The central theme in this work is the application of heterogeneous photocatalysis to the destruction of organic contaminants in industrial waste discharges such as; produced water from oil rigs, and dyes from textiles industry wastewater streams.

1.3 Aims and Objectives

In this research, a new photoreactor designed at the Centre for research in Energy and the Environment (CRE+E) at the Robert Gordon University, (WO2005/033016 A1) based on a slurry-continuous flow reactor configuration was studied as part of the optimization process of a novel photocatalytic reactor design. The reactor configuration combines the high surface area contact of catalyst with pollutant of slurry reactor with a higher illumination of catalyst surfaces. The novel reactor configuration employs a commercial pellet TiO_2 catalyst as against the traditional

powder TiO₂ catalysts currently used and reported by most researchers in the field of photocatalysis. The use of powder TiO₂ catalyst in a conventional slurry reactor even though gave a better degradation results will require the recovery of the fine catalyst particles after the degradation process. This adds to the cost and time required for the process and in a large scale application could be a major drawback for the process.

The novel reactor design has greater potential for scale-up. The reactor configuration reduces the light passage through the reaction liquid; this is advantageous because, when light approaches the catalyst through the bulk liquid phase, some radiation is lost due to absorption in the liquid. In particular, this effect is more pronounced for highly coloured pollutants as they are strong UV absorbers and will therefore significantly screen the TiO₂ from receiving UV light and possible total reactor illumination.

The main objective of this work was the evaluation and testing of a novel photocatalytic reactor for the degradation of model organic compounds in water using a commercial pellet TiO₂ catalyst.

Methylene blue was used to determine the adsorption capacity of the commercial pellet TiO₂ catalyst and the optimum catalyst loading of the reactor. MB is a thiazine (cationic) dye; it is one of the most important basic dye, used in different applications such as dyeing and printing industries. MB dye was chosen as a model organic pollutant to optimize the novel photocatalytic reactor because of its wide use and because the removal of dye from industrial wastewater constitute an acute problem. Furthermore, extensive research into the degradation of MB in aqueous TiO₂ is widely investigated and its behaviour under different experimental conditions are widely reported. This aspect was analyzed in a batch configuration of the reactor.

Congo red and acridine orange dyes were also used as a model (recalcitrant) organic pollutant to evaluate the photocatalytic capability of the novel reactor. They were used as a representative of a class of pollutants in wastewater resistant to biodegradation. Reaction mechanism and kinetics of photodegradation of target organic compounds, congo red dye, acridine orange dye, and real produced water

sample was investigated in a continuous flow configuration, typical of industrial processing.

CHAPTER 2

LITERATURE REVIEW

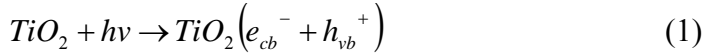
2.1 Heterogeneous photocatalysis

Heterogeneous photocatalysis entails the use of a solid photocatalyst (usually a semiconductor) in contact with either a liquid or gas. It couples low-energy ultraviolet light with semiconductors acting as photocatalyst, and it involves the generation of highly reactive oxidative species produced by several pathways, including reactions with H_2O_2 and O_3 with or without ultraviolet (UV) irradiation. In this process, in situ, degradation of trace of organic substances is achievable. Reactants in heterogeneous photocatalysis in water are naturally occurring species such as oxygen, water molecule, and hydroxide ions (OH^-) as compared to chemically supplied reactants (such as hydrogen peroxide and ozone) required for other advanced oxidation process. The carbon-containing pollutants are oxidized to carbon dioxide if left long enough while the other elements bonded to the organic compounds are converted to anions, such as nitrates, sulphates, or chlorides.

Literature has established that practically any pollutant that includes aliphatic, aromatics, dyes, surfactants, pesticides, and herbicides can be completely mineralized by this process into harmless substances [30]. The first clear recognition and implementation of photocatalysis as a method for water purification was conducted by Ollis and co-workers [31] in the photomineralization of halogenated hydrocarbon contaminants in water, including trichloroethylene, dichloromethane, chloroform, and carbon tetrachloride, sensitized by TiO_2 . Since then, numerous studies [10, 16, 32-45] have shown that a great variety of dissolved organic compounds could be oxidized to CO_2 by a heterogeneous photocatalysis technique. Most of the early studies [46-50] of heterogeneous photocatalysis were done to investigate the effect of various parameters such as ;(a) catalyst loading, (b) initial concentration of solute, (c) light intensity, (d) recirculation rate, (e) pH of the solution, (f) partial pressure of oxygen, and (g) temperature, influence the rate of degradation of compounds through heterogeneous photocatalysis.

2.2 Reaction mechanisms of TiO₂ photocatalysis

Ultraviolet (UV) illumination with radiation ($\lambda < 380\text{nm}$) of energy higher than the band gap energy of TiO₂ ($E_g \cong 3.2\text{eV}$, for anatase phase) induces electron and hole formation in the conduction and valence bands of the semiconductor, respectively. These charges carrier species can recombine, releasing the absorbed energy as heat, or undergo interfacial transport to the surface. These holes can then be trapped by intrinsic sub-surface traps ($Ti^{IV} - O^2 - Ti^{IV}$). Alternatively, the photogenerated holes and the electrons can also be captured by extrinsic surface traps via interfacial electron transfer with adsorbed molecules (electron donors and acceptors, respectively). In the presence of water, hydroxyl radical (OH^\bullet) formation occurs on the semiconductor surface due to hole trapping by interfacial electron transfer. During the photocatalytic process, other oxygen containing radicals are also formed including the superoxide radical anion ($O_2^{\bullet-}$) and the hydroperoxide radical (HO_2^\bullet). Both hydroxyl radical attack and hole oxidation have been shown to be the primary pathways for the oxidation reaction [51]. The hydroxyl radical is the most reactive of the oxidizing agents (see Table 2-1) and can be generated via several pathways:



Absorption of a photon in near UV range by the TiO₂ promotes an electron in the conduction band, which produces a hole h_{vb}^+ in the valency band (equation 1). Subsequent migration to the surface through diffusion or drift, followed by oxidation

of adsorbed water by the generated hole (equation 2.) to produce OH^\bullet radical. Photogenerated hole (h_{vb}^+) also oxidized adsorbed hydroxide ions OH^- (equation 3) and the transient formation of hydroperoxide via equation 4 and subsequent decomposition via equations (5-8) complete the hydroxyl radical generation sequence. As can be seen from equations (4-8) molecular oxygen plays a dual role in heterogeneous photocatalysis by creating an oxidative species, the super oxide radical ($O_2^{\bullet-}$) acting as an electron acceptor to prevent the electrons and holes from recombining. These functions are very important in establishing an efficient photocatalytic system; it has been shown that with an increase in oxygen concentration, there is a subsequent increase in the reaction rate of contaminant degradation [48]. Decomposition of H_2O_2 (Equation 8) by the super oxide radical ($O_2^{\bullet-}$) leads to the formation of the hydroxyl radical (OH^\bullet).

Species	Relative Oxidation Power
Hydroxyl radical	2.06
Singlet oxygen radical	1.78
Hydrogen peroxide	1.31
Perhydroxyl radical	1.25
Chloride dioxide	1.15
Chlorine	1.00

Table 2-1. Oxidation power of various species relative to Chlorine [52].

Several mechanisms have been proposed to account for the initial steps of the photodegradation of organic species with TiO_2 as a photocatalyst. One mechanism suggests that the oxidation of organic compounds is first initiated by free radicals, e.g. hydroxyl radical (OH^\bullet) formed in the aqueous solution, which are mainly induced by the electron-hole (e^-/h^+) pairs at the photocatalyst surface [48, 52]. Another mechanism states that the organic compounds is first adsorbed on the photocatalyst surface and then reacts with excited superficial e^-/h^+ pairs or OH^- to form the final products [53]. A variety of reaction mechanisms depends on both surface adsorbed and solution phase species, resulting in different kinetics of photodegradation [54].

Adsorption of the organic pollutants is generally considered to be an important parameter in determining degradation rates of photocatalytic oxidation process [54], however, only a few studies on the kinetics of organics adsorbed on the photocatalyst have been reported [55-57].

2.3 Photocatalytic Reactor Technologies.

The different types of photoreactor generally employed in photodegradation studies can be classified into four (4) groups, based on the manner in which the catalyst is used, on the arrangement of the light source and the reactor vessel. They are; (i) slurry-type in which the catalyst particles are in suspension form, (ii) immersion-type with lamp(s) immersed within the reactor, (iii) external-type with lamps outside the reactor, and (iv) the distributive-type with the light distributed from the source to the reactor by optical means, such as reflectors and light conductors or optical fibers [16].

A number of photocatalytic reactor designs have been patented in recent years, the majority of them are a variation of the slurry reactor and the classical annular reactor of immersion or the external-type in which the catalyst is immobilized on the reactor wall, on pipes internally, on ceramic membrane, on glass wool matrix between plates, on porous filter pipes, and on glass fiber cloth. However, all these reactor designs are limited to small scales application due to low light utilization efficiency and mass transport limitation within the reactor [58]. The only way to apply these systems to large-scale applications is by using large numbers of multiple units which consequently pushes the cost of the application of the technology higher. The central problem in the photocatalytic reactor design is now focused on a uniform distribution of light to a large surface area of the catalyst [46].

In order to meet the scale-up reactor design challenges, a number of different types of photocatalytic reactors have been developed and used in research or pilot plant studies. Examples of these reactors include the annular photoreactor [6, 59-61], the packed bed photoreactor [62], the photocatalytic vortex reactor [63], the TiO₂-coated fiber optic cable reactor [63, 64], the falling film reactor [63-66], the thin-film-fixed-

bed sloping plate reactor [63-67], rotating disk photocatalytic reactor[68], and the swirl-flow reactor [69]. However, there is still a need for the improvement of current photocatalytic reactors or the development of new types of such reactors with the objective of commercializing this technology.

Evaluation and testing of a novel photocatalytic reactor is an objective of this thesis and the reactor design applied in this study is patented (W02005/033016A1). This study focuses on the characterization, and evaluation of a novel Slurry-Continuous-Flow Reactor design for the destruction of organic pollutants in water. It is anticipated that the process will be suitable for the degradation of various organic contaminants which do not lend themselves to purification using conventional adsorption (e.g. activated carbon adsorption), and oxidation (e.g. O₃) processes, as well as for disinfection.

The new reactor design concept provided a high ratio of activated catalyst to illuminated surface of a slurry reactor and a high density of active catalyst in contact with the liquid to be treated inside the reactor, without the necessary post-filtration separation associated with slurry reactor with the deployment of a commercial pellet TiO₂ catalyst. The novel reactor design has greater potential for scale-up. The reactor configuration reduces the light passage through the reaction liquid; this is advantageous because, when light approaches the catalyst through the bulk liquid phase, some radiation is lost due to absorption in the liquid. In particular, this effect is more pronounced for highly coloured pollutants as they are strong UV absorbers and will therefore significantly screen the TiO₂ from receiving UV light [20, 46, 70] and possible total reactor illumination.

Matthews studied the photocatalytic degradation of 22 organics both in TiO₂ aqueous suspensions in a spiral reactor [10] and over immobilized TiO₂ thin film [44]. For the suspended TiO₂ experiments; phenol, 4-chlorophenol, and benzoic acid photocatalytic degradation using a spiral reactor, with a pump to circulate the suspension was reported. A zero-order rate at high concentration and a first-order rate at low solute concentration were observed. No significant effect of circulation of the suspension on the rate of degradation was reported. He assumed no mass transfer limitation with the suspended reactor configuration. In the degradation of organic impurities in water

using a thin film reactor, Matthews [44] reported that in a continuous recirculation mode, the destruction rate of phenol, 2-chlorophenol (2-CP), and 4-chlorophenol (4-CP) obeyed approximately first-order kinetics. The reaction time for a 50% destruction of phenol, 2-CP and 4-CP using 500ml of 10 μ M solutions was 7.2, 8.2, and 8.7 min⁻¹ respectively.

Chen and Ray [2] studied the photocatalytic degradation of 4-nitrophenol in a swirl-flow reactor with suspended TiO₂ catalyst with recirculation. They reported an initial pseudo-first-order rate with respect to the initial concentration. The rate of degradation increases as catalyst loading is increased and reaches a plateau at 2 g/L. The degradation rate was observed to be quite slow at both high and low pH value and concluded that the best pH is between 5.6 to 6.4. The rate of degradation was reported to increase as the partial pressure of oxygen is increased and a plateau was reached at about 0.4 atm. No significant change was observed with temperature adjustment.

In the work of Inel and Okte [50], photocatalytic oxidation of malonic acid was investigated, in the presence of TiO₂ using a gas recycling reactor made of a pyrex tube. The possible photocatalytic oxidation of the malonic acid to give CO₂ was followed and the initial kinetics of CO₂ photogeneration was studied. The dependence of CO₂ formation on the TiO₂ concentration was followed in the range 0.1-3.1 g/L. They reported CO₂ formation increases with increasing TiO₂ concentration up to 0.8 g/L. With a further increase in TiO₂ concentration, the formation of CO₂ was reported to reach a limiting value. The rate of CO₂ formation was also reported to be affected by pH values and reaches a plateau at pH = 9. They reported in their experiments that the rate of malonic acid degradation (CO₂ generation) increased with temperature.

Rideh et al., [70] investigated the photocatalytic degradation of 2-chlorophenol in a cylindrical annular pyrex reactor with external recirculation. They reported a decrease in rate of degradation with an increase of initial concentration, but reported an increase in degradation rate with catalyst loading (plateau was reached at a catalyst loading of 0.2 g/L). Rate of degradation was observed to be proportional to the light intensity. They observed a low rate of degradation in acidic region, a constant rate in the neutral region and a higher rate of degradation in the basic region. The rates were

observed to increase non-linearly as the partial pressure of oxygen was increased and no significant effect was observed with temperature variation.

Dijkstra [72] studied the photocatalytic degradation of formic acid in suspension and immobilized system, with and without oxygen addition. They reported that in the immobilized system, oxygen addition to the reactor appeared to increase the efficiency, not only because oxygen acts as an efficient electron scavenger, but also due to increase mass transfer in this two-phase reactor. The immobilized system was reported to have a higher efficiency compared to the suspended system. The addition of oxygen to the immobilized system appeared to increase the quantum yield with a factor 4, whereas the addition of oxygen to the suspended system did not have any appreciable effect on rate of degradation. The optimal reactor configuration has the highest possible illuminated specific catalyst area fixed on a support material which uses the light efficiently.

Mehrotra et al., [73] reported a systematic analysis carried out to distinguish kinetic and transport limited regimes for photocatalytic degradation in a TiO₂ slurry system using benzoic acid as a model compound. Experiments were performed to investigate the effect of catalyst loading, circulation rate, initial concentration of solute, and light intensity on the degradation rate to differentiate the 'kinetic' regime (in which the observed rate is governed by kinetic dependences) from the 'transport' regime (internal mass-transfer limitation- particle agglomeration effect and light transport limitation- shielding effect). It was reported that there is no external mass transfer limitation (the rate is not affected by the recirculation rate) at lower catalyst loading, but at high catalyst loading, there was both internal mass transfer limitation (agglomeration) and light limitation (shielding effect).

The domain of kinetics, the domain of internal mass transfer limitation (particularly agglomeration effect) and the domain of light transport limitation (shielding effect) were distinguished. Experimental results demonstrated a significant difference in the rate value between the optimum catalyst loading regime and the kinetic regime. The

true kinetic dependency of the photocatalytic degradation rate on light intensity and the substance initial concentration were determined.

Yatmaz et al., [67] reported a new type of photocatalytic reactor, the spinning disc reactor (SDR) which was used to degrade an aqueous solution of 4-chlorophenol and salicylic acid. The efficiency of the photocatalytic process was reported to depend on the type of UV source used. Lamps supplying a shorter wavelength UV radiation were reported to be more efficient than those whose emission lies mainly in the near UV region. The characteristics of the turbulent liquid film produced in the SDR reduce the influence of mass transfer on the overall photocatalytic process.

Hong Fei et al., [74] investigated the TiO₂ catalyzed photodegradation of 1, 2-dichlorobenzene (DCB) from a dilute water stream using a mixed slurry reactor and a semi-batch reactor with continuous feed recycle with titanium dioxide immobilized on inert supports (quartz and low density polyethylene, LDPE). They reported that increasing the pH of the solution increased the initial rate of photodegradation of DCB. Added oxidant (hydrogen peroxide) did not have any appreciable effect on the degradation of DCB. The steady state removals and apparent rate constants were obtained for the plug-flow reactor with different supports and compared under similar conditions.

The titania supported on LDPE showed a better rate of photocatalysis than titania supported on quartz, although the titania film thickness on LDPE was five times lower than on quartz. The fractional removal of DCB using titania on LDPE was reported to be (43.6 ± 8.4) %, the efficiency under the same conditions for titania on quartz was reported to be (25.3 ± 4.0) %. The respective rate constants were reported to be 0.042 and 0.022 min⁻¹. The differences in observed rates was reported probably due to differences in the binding characteristics between titania on LDPE and quartz, better surface coverage of titania due to surface conditioning of LDPE as opposed to the quartz surface used without pretreatment, and possibly even different electron – hole interactions on the two substrates. The modification of titanium surface by adsorption of a non-photodegradable polyfluorinated surfactant vastly improved the rate of DCB degradation on both LDPE and quartz. The rate of photodegradation in the

immobilized tubular reactor was mass transfer controlled for the flow regime investigated. The steady state degradation rate was reported to be proportional to the radiant flux within the range (4-16) mW/cm².

In another study, Hong Fei and Kalliat [75] investigated the photodegradation of two polycyclic aromatic hydrocarbons (PAHs), phenanthrene (PHE) and pyrene (PYR) from a dilute water stream, using an external lamp, annular photocatalytic reactor with titanium immobilized on quartz tube. Thin film geometry was used to obtain the mass transfer coefficients and intrinsic reaction rate constants for the two compounds on immobilized titanium (Degussa P-25) particles. In their study, they reported that beyond a feed velocity of 7cm³/min, the conversion was solely reaction rate controlled and was not subject to mass transfer limitations from the aqueous phase to the immobilized titanium film.

The effect of PHE concentration upon fractional conversion was studied for the range between 100 and 1200 $\mu\text{g} / \text{L}$. It was reported that the fractional conversion did not show any discernible difference or trend in the range of concentrations investigated. Nothing that the maximum concentration used was the aqueous solubility of PHE, and that the photodegradation of PHE is not a function of the concentration. The overall reaction rate constant was reported to be independent of the feed concentration as large as the saturation aqueous solubility of the two compounds. However, the conversion was reported dependent on the ultraviolet (UV) light illumination intensity at the reactor. The reaction rate constant was reported to increased linearly with the UV illumination intensity up to approximately 2 mW/cm² and thereafter showed smaller changes up to 8 mW/cm². The quantum efficiency of the reactor was observed to range from 3.7×10^{-5} to 2.7×10^{-4} which was somewhat low because of the low concentration of the aqueous solutions. The overall reaction rate constant was reported to be 1.6 times larger for pyrene than for phenanthrene.

Maya Nasir et al., [76] investigated the TiO₂ photocatalysed oxidation of marine crude oils spilled using buoyant hollow fly-ash-derived cenosphere as catalyst carriers. They reported that, the rate of photoassisted oxidation is light limited only at

levels of solar near-UV irradiance, below those in normal direct sunlight irradiance (below 25W/m^2) but varied only mildly with irradiance in the $(25 - 45)\text{W/m}^2$ range. In direct sunlight, the rates can be mass transport dependent. Both fresh crude oil spills and their non volatile residues are oxidized in the photoassisted oxidation process. Waves were reported to enhance the cleanup process by improving mass transport (imitating agitation of the liquid). The degradation rate increases upon increase of the cenosphere: oil mass ratio. The degradation rate was also reported to vary only mildly for the different crude studied i.e. Arab Heavy, Arab Light, Basrah Light, and Texaco Bruce No.1.

Zahraa [4] studied the photocatalytic degradation of herbicide atrazine using suspended titanium dioxide as catalyst. Atrazine was reported to be partially degraded by the photocatalytic process. The kinetics of degradation obeys satisfactorily the Langmuir-Hinshelwood model from which an adsorption constant was determined. The rate of degradation was found to be enhanced by the addition of persulphate ions.

Inoannis et al., [77] investigated the photocatalytic degradation of azo dyes containing different functionalities using TiO_2 in aqueous solution under solar and UV irradiation. They reported that the effective destruction of azo dyes belonging to different chemical groups is possible by photocatalysis in the presence of TiO_2 suspension with ultra violet (UV), visible or solar light. The mechanism of the photodegradation oxidation followed a Langmuir-Hinshelwood model and was dependent on several factors such as, dye concentration, mass of catalyst, wavelength, radiant flux and the addition of oxidants or the presence of natural occurring substances (humid substances and /or inorganic ions). The degradation of dyes depends on pH, catalyst concentration, substrate concentration and the presence of electron acceptors such as hydrogen peroxide and ammonium persulphate besides molecular oxygen.

Zhang et al., [78] investigated sodium benzene sulfonate (BS) decomposition in aqueous TiO_2 dispersions under highly concentrated solar light illumination to examine the photocatalytic characteristics of a parabolic round concentrator (PRC) reactor to degrade the pollutant without visible light absorption. The effect of such

operational parameters as initial concentration of BS solution, oxygen purging and TiO₂ loading on the kinetics of decomposition of BS were investigated. They reported that an effective photodegradation necessitated a suitable combination of initial volume and concentration of BS solution. Relative to atmospheric air, oxygen purging significantly accelerates the degradation process at high initial concentration of BS (0.40mM or 1.0mM). Optimal TiO₂ loading was reported to be 9 g/L, greater than previously reported by other researchers. Elimination of TOC follows pseudo first-order kinetics in the initial stages of the photodegradation process.

Considering the difficulty of quantum yield measurements, Zhang et al., reported the use of phenol as a standard actinometer to assess the relative photonic efficiency of the photodegradation of BS against phenol. The photodegradation of phenol and BS was carried out under identical experimental conditions. Based on the degradation rate constants for BS and phenol, the relative photonic efficiency for BS was determined to be $\zeta_{rel.} = 1.01$. The $\zeta_{rel.}$ infers that both BS and phenol are decomposed at the same rate, both molecules contain only one benzene ring and ring-opening occurred at identical rates.

Michael [79] reported a comparative study of the degradation by photocatalysis and photo electrochemical processes of 4-chlorophenol using TiO₂ thin film prepared by chemical vapour deposition on SnO₂ coated glass. He reported a low quantum yield arising from the very fast recombination of photo-generated electrons and holes with lifetimes of between picoseconds and nanoseconds. He concluded that holes have a very limited time to react with any target substance and photo-energy is simple converted to heat without efficient chemical reaction. He stated that to try and reduce the electron-hole recombination, an electric field can be applied across the TiO₂ film to promote spatial separation of photo-generated electron-hole pair, with an external circuit providing a sink for the electrons.

Chang et al., [80] reported the thin-film photocatalytic model used to investigate the effect of catalyst properties on the photodegradation of organics. The properties investigated included adsorption capacity, diffusion in the catalyst, UV properties and

film thickness. The results of model simulation show that the effect of catalyst properties on the degradation of organics is highly non-linear. They reported that there is an optimal film thickness that yields a maximum rate of photodegradation. The model not only provides insight into the effect of liquid-film transfer, adsorption, diffusion and photocatalytic reaction in a thin-film mechanism, but also can be used as a tool to assist the design of a thin film photocatalyst. A mathematical model was developed to incorporate these mechanisms for the photodegradation of organic molecules in a batch reactor. The model was verified using the data of 4-chlorophenol degradation obtained from literature.

Generally, it has been demonstrated from these studies that: the photocatalysed degradation rate depends on the initial concentration of the solute. Although at high concentration the observed rate is independent of the solute concentration (zero-order dependency), at low concentration it shows first-order dependence, while at some intermediate concentration it follows a Langmuir-type dependence [34]. The degradation rate increases with catalyst loading, reaches a maximum at some optimum catalyst loading and then decreases. The researchers attributed the decrease of rate at high catalyst loading to the obstruction of light transmission and defined it as the 'shielding effect' [81].

The reaction rate is proportional to the light intensity, but at higher intensity the rate becomes proportional to the square root of the light intensity. As the light intensity increases, so does the recombination rate of the hole and electron [49]. The effect of variable flow rates on degradation has also been studied. Generally, no significant influence of variable flow rates on degradation rate has been reported for slurry system [20, 82]; hence all catalysts reached the illumination zone in slurry reactors. Although an increase in degradation rate due to circulation rate was reported by Inel et al.,[50].

In most cases, it was found that pH has a direct impact on the degradation rate. It has been observed that pH affects the surface properties of the TiO₂ catalyst, and the degradation rate [47]. The rate increases with the increase of oxygen partial pressure. The typical explanation is that oxygen acts as an electron-scavenger, thus reducing the rate of electron-hole recombination [48]. The effect of temperature is not so

significant in most of the studies reported, possibly because primary photon absorption is not temperature dependent.

CHAPTER 3

METHODS AND MATERIALS

3.0 Methods and Materials

3.1 Reactor Set-up

Figure 3.2 illustrates the reactor set up. The photocatalytic reactor consists of (i) three serially connected rotating cylindrical vessels (570mm length and 94mm i.d.) with weir-like paddles constructed along the longitudinal length of the vessels and (ii) an external illumination source. Rotation of the cylindrical vessels was provided by three 12 V electrical motors and illumination was provided by six low pressure 36 W mercury UV tubes, (Philips Technology). The lamps had an emission output of 330-400 nm with a maximum at 350 nm wavelength (Figure 3.1). The tubes were mounted in pairs, adjacent to each other on a reflective mirror, and enclosed in a wooden box to provide control over exposure to ambient light. The lamps were cooled by air flowing freely within the openings between the reactor vessels and the UV tubes.

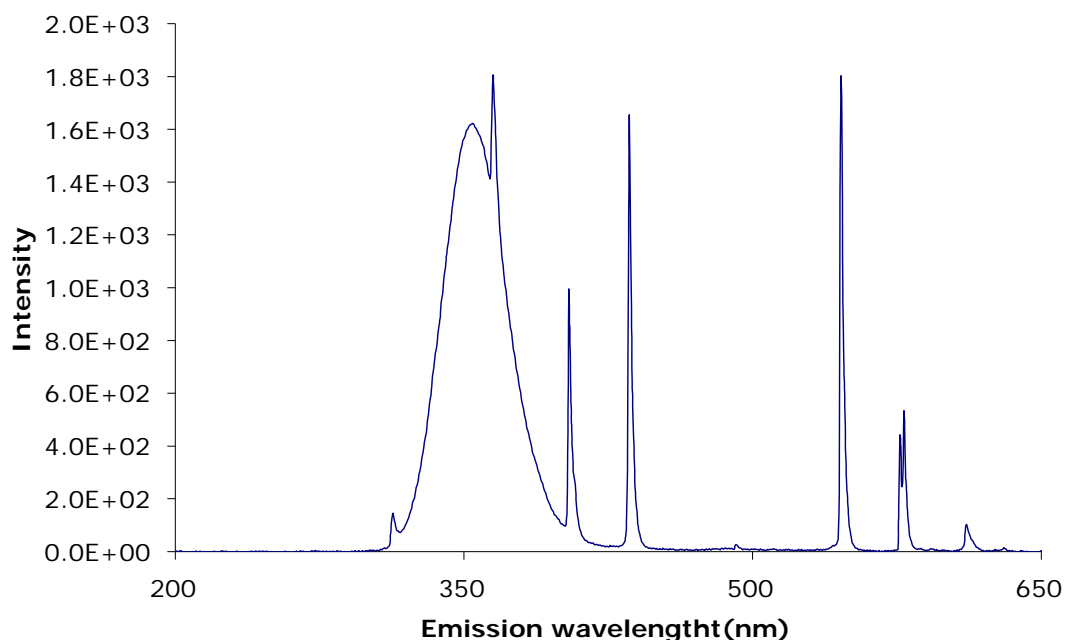


Figure 3.1: Emission spectra of UV lamp (Philips PL-L 36 W), maximum emission at 356 nm.

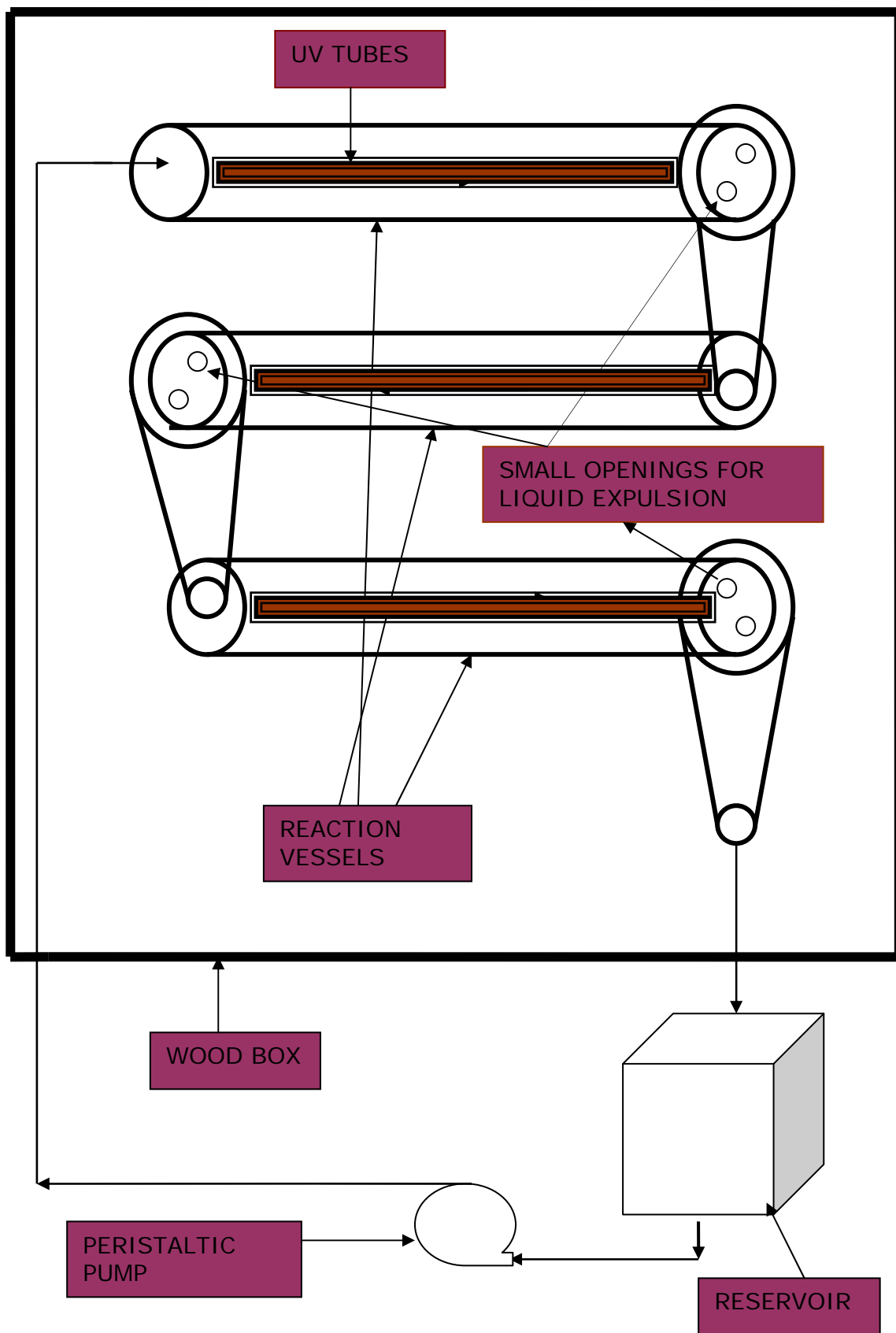


Figure 3.2. Schematics of the photoreactor configuration.

The experiments were performed in the novel reactor in two modes: (1) batch configuration, with catalysts suspended in the aqueous solution to be degraded and the aqueous suspension agitated and irradiated. (2) Semi-batch with catalysts suspended in the aqueous solution to be degraded and the aqueous suspension agitated and irradiated, with recirculation of the aqueous solution between the three reaction vessels and the reservoir.

A known volume of solution to be treated, methylene blue was placed inside an amber bottle (2.5 L) as a reservoir. An amber bottle was used to eliminate ambient light irradiation, since MB can be degraded by ambient light within the laboratory (depending on concentration and ambient light intensity). The solution was transferred from the reservoir with a peristaltic pump (Autoclude) to the top vessel and the reaction vessel rotated to expel the liquid down to the next reaction vessel until there was fluid in all three vessels. The fluid then flowed back to the reservoir where the pump returns it back to the top vessel in a continuous flow manner.

The reactor system also includes a control system for angular speed adjustment. The body of the reaction vessels were fabricated from a perspex material which is very transparent, to allow light transmission through it (% T= 90) [83]. One side of the reaction vessel was open to the atmosphere and during the course of rotation, a thin film of liquid and catalyst was removed from the aqueous suspension with the aid of the weir-like baffles constructed alongside the inner walls of the reaction vessel. This thin film of water and catalyst was exposed to air and UV irradiation while above and below liquid level. The liquid film returns to the aqueous solution as the reaction vessels rotate in a continuous pattern.

Light rays entering the vessels through one end are repeatedly internally reflected down the length of the vessel and at each reflection come into contact with the catalyst present.

3.2 Materials

Methylene blue, ~ 85%, (remaining 15% primarily salt), acridine orange, ~ 90 %, (remaining 10% ZnCl₂), and congo red, ~ 54 %, were purchased from Sigma- Aldrich and used in aqueous solution (Milli Q water). Titanium Dioxide (TiO₂) in pellet form was purchased from Sachtleben Chemie of Germany (Hombikat KO1) and used as purchased; the composition was reported to contain about 80 % anatase and 20 % rutile. Specific surface area (BET) = 95 m²/g, primary particle size ~ 15nm, mean pore diameter (N₂) ~ 150 Å, pH~ 5.5.

3.3 Methods

3.3.1 Batch Degradation Experiment

A stock solution of methylene blue (MB) (10μM) was prepared and used for all experiments. The TiO₂ pellet catalyst was weighed and placed in the reaction vessel. To start the experiment, the feed solution was pumped (Auto Clude Peristaltic pump) from the reservoir to the reaction vessel containing the catalyst. MB (10μM, 1L) was added into the reaction vessel containing catalyst. The motor was switched on and the aqueous suspension continuously agitated for 60 min in the dark. This was sufficient time for the reaction to reach equilibrium. Samples were drawn at 5 min intervals, centrifuged with Henderson T121 Centrifuge for 15 min at 6000 rpm to eliminate any suspended TiO₂ particles. The change in absorbance of MB was monitored at different time intervals using UV-Vis Spectrophotometers (Perkin Elmer Lambda 950). Absorption spectra of samples were recorded between 200-750 nm and maximum absorbance $\lambda_{\text{max}} = 666$ nm was used to calculate the concentration of MB. Two other conditions were then investigated, the first was under UV illumination and the second was without any catalyst present.

3.3.2 Continuous Flow Experiment

3.3.2.1 Dark Adsorption

For the continuous flow dark adsorption experiment, the solution was transferred into the reaction vessels containing the pre-weighed catalysts, the electrical agitation motor was switched on and the aqueous suspension was continuously agitated and recirculated for the 60 min experiment duration. The aqueous suspension flowed through the three reaction vessels and back to the reservoir where it was returned to

the top vessel for another round of recirculation. Samples aliquot (15 mL) were drawn at 5 min interval for 60 min, centrifuged (Henderson T121) for 15 min at 6000 rpm to eliminate any suspended TiO_2 particles and analyzed with UV-visible spectrophotometer.

3.3.2.2 Control Experiment

For the continuous flow control experiments, after the complete transfer of the solution to be treated into the reaction vessel (without any catalyst loaded), the motor was switched on to allow the aqueous solution flow through all the three serially connected reaction vessels and exit back to the reservoir. The illumination light was then switched on and the solution was agitated for the next 30 min. Samples were taken at 5 min intervals during the irradiation period and analyzed with UV-Vis spectroscopy for changes in MB concentration.

3.3.2.3 Degradation Experiment

For the continuous flow degradation experiments, similar procedure for the control experiment was applied except that various loads of TiO_2 catalyst were placed in the reaction vessels.

3.3.3 Analytical Methods

3.3.3.1 Calibration Plots

A standard stock solution of each pollutant was prepared at various concentrations. Absorbance in the UV and visible range was measured with a Perkin Elmer (Lambda 950) UV-visible spectrophotometer. Absorbance spectra of samples were recorded between (200-750) nm. The absorption spectra of MB are shown in Figure 3.3, with three major absorption peaks observed at 293, 613, and 666 nm. The maximum peak at 666 nm was used to correlate the various concentration of MB.

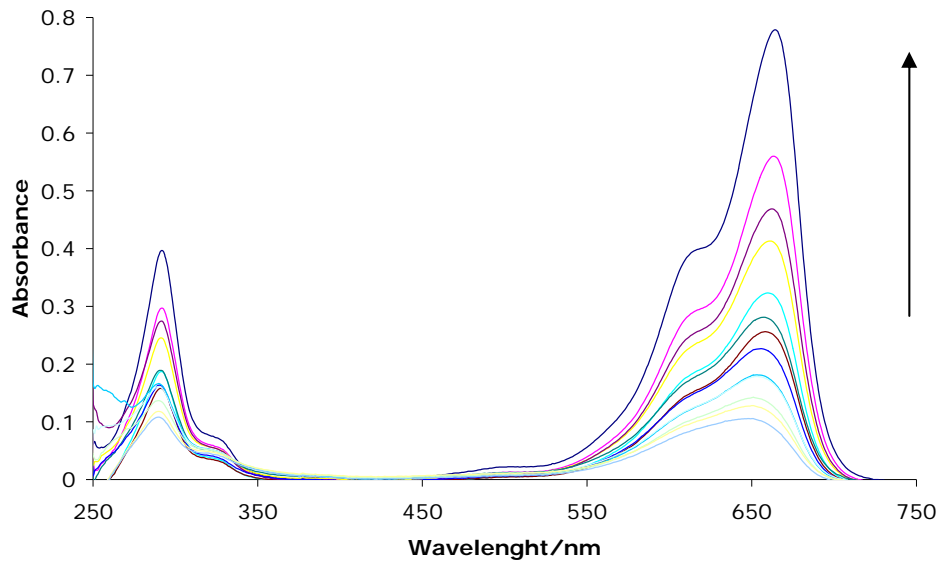


Figure 3.3: Methylene Blue absorption spectra over (250-750) nm wavelength and maximum absorbance at 666nm.

The effect of pH on MB absorbance spectrum was not investigated in this study. The changes in absorbance spectrum of MB monitored at different concentration were plotted against absorbance intensity to generate the calibration curve (Figure 3.4).

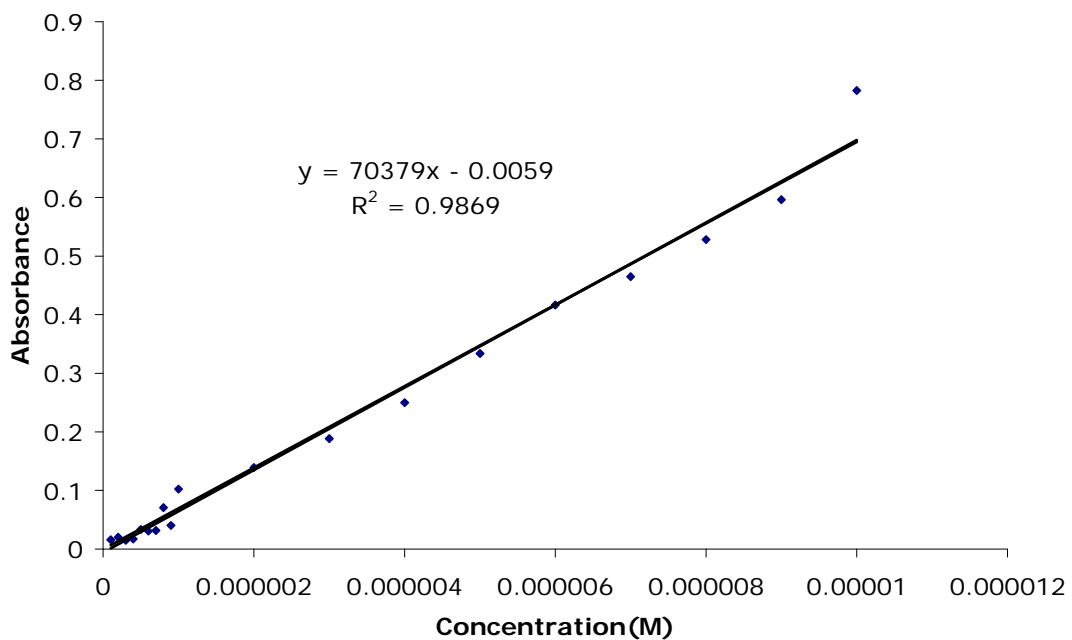


Figure 3.4: Methylene Blue Calibration Plot at 666 nm wavelength.

The calibration curve was subsequently used to determine the changes in concentration with time of samples from the experimental runs. The molar extinction coefficient value of MB obtained from the slope of the calibration plot $\epsilon_{666} = 70,379 M^{-1} / cm$. A similar procedure was adopted for acridine orange (AO) (see appendix, figure A1&A2) and congo red (CR) (appendix, figure A3&A4). Each of the calibration plots was obtained using the maximum absorbance reading of the absorption peak recorded between 250-650 nm wavelengths with maximum absorbance at 666 nm, 497 nm and 503 nm for MB, AO, and CR respectively.

3.3.3.2 Total Organic Carbon (TOC) analysis

Photocatalytic degradation of dye solutions were primarily monitored by the extent of decolourization of the residual dye solution using UV spectroscopy, but the extent of degradation calculated from UV adsorption does not indicate the degree of mineralization. Oxidative mineralization was therefore, measured by the decrease in TOC. TOC measurement was therefore a secondary analysis tool for the dye degradation experiments while it is the main tool for sample produced water analysis.

Two types of carbon are present in water; organic and inorganic carbon. Organic carbon (TOC) bonds with hydrogen or oxygen to form organic compounds. Inorganic carbon (IC or TIC) is the structural basis for the inorganic compounds such as carbonates and carbonate ions. Collectively the two form of carbon are refereed to as total carbon (TC) and the relationship between them is expressed; $TOC = TC - IC$.

The TOC was measured with a Shimadzu TOC-VCPH/CPN analyzer by directly injecting the aqueous solutions after centrifugation. The analytical procedure requires adjusting the aqueous sample pH to below 3 in order to convert major sources of inorganic carbon, carbonate and bicarbonate ions, to carbon dioxide. The carbon dioxide is purged from the sample with an inert gas, dried, and sent to a calibrated non-dispersive infrared analyzer (NDIR) for carbon dioxide analysis. The total

inorganic carbon in the aqueous sample is related to the carbon dioxide content which is measured by the NDIR analyzer.

Once the inorganic carbon has been removed from the sample, the organic carbon is oxidized in the presence of an oxidant and UV radiation, again, forming carbon dioxide. The carbon dioxide, as with the total inorganic carbon (TIC) is purged, dried and measured by the NDIR analyzer.

Chapter 4

Results and Discussion

4.0 System Optimization

The novel photocatalytic system was optimized with respect to flow rate, titanium dioxide loading, batch/continuous flow pattern and number of reaction vessels using methylene blue (MB) as a model pollutant. For each test of the system, one parameter was varied while the others remain constant. The adsorption and degradation capability of the system was tested under each set of conditions. The optimum system parameters were chosen based on the ability to reduce the initial concentration of MB in the shortest amount of time.

MB dye was chosen as a model organic pollutant to optimize the novel photocatalytic reactor because of its high molar absorptivity (ϵ) which allows the rate of decomposition to be monitored by UV spectroscopy, even for very dilute solutions [84]. MB is one of the most widely used dye for colouring among all other dyes of its category and its degradation under different experimental conditions is widely reported, which allows for comparison of its degradation with the novel photocatalyst. UV spectrophotometry was therefore used for determining the extent of MB dye degradation by photocatalysis and MB adsorption on the TiO_2 catalyst.

Absorbances of both the chromophoric group and aromatic rings in the dye were measured at the respective wavelength. The degradation efficiencies were calculated by monitoring the initial absorbance prior to reaction and the absorbance recorded following the reaction period at time t .

4.1 Adsorption Equilibrium

Adsorption of organic pollutants is generally considered to be an important parameter in determining the degradation rates of photocatalytic oxidation [68]. Adsorption of MB on the surface of TiO_2 strongly affects the degradation process [85]. Several mechanisms have been proposed to account for the initial steps of the photodegradation of organics with TiO_2 as a photocatalyst. One mechanism suggested that the oxidation of organic compounds occurs following adsorption of the organic

compounds on the photocatalyst surface and then reacted with excited superficial e^-/h^+ pairs or OH^\bullet to form the final products [37].

The adsorption of methylene blue (MB) on TiO_2 pellet catalysts at various loadings (30, 60, 90, 120, 150, 180 and 200g) are shown in figure 4.1. The amount of MB actually adsorbed was calculated by subtracting the final solution concentration from the initial concentration. The optimum catalyst loading of the system (in terms of adsorption) was determined by calculating the amount of MB adsorbed at equilibrium since maximum adsorption occurs at equilibrium. The amount of MB adsorbed at equilibrium Q_e (mg/g) was obtained as follows:

$$Q_e = \frac{(C_o - C_e)V}{W} \quad (9)$$

where C_o and C_e are the initial and equilibrium liquid-phase concentrations of MB (mg/L) respectively. V is the volume of solution (L) and W is the amount of adsorbent (TiO_2) used (g).

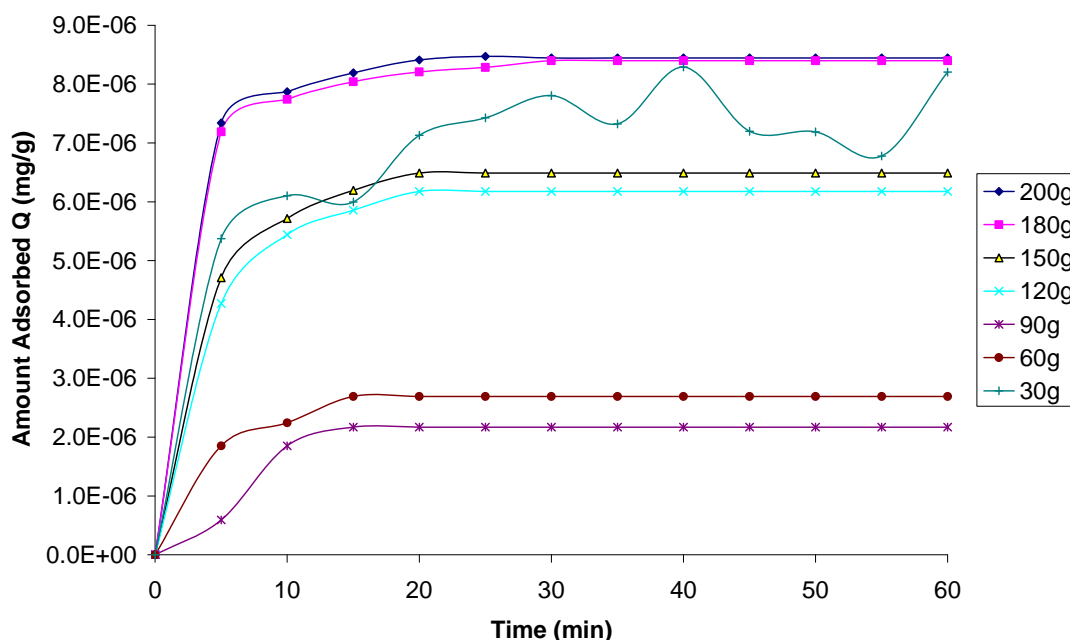


Figure 4.1: Adsorption of MB on TiO_2 pellet for initial concentration $10\mu M$ for various catalyst loadings.

The results show a gradual increase in the amount of MB adsorbed as the catalyst loading was increased until an apparent optimum loading of 180g for the experimental conditions investigated. This can be attributed to increased TiO₂ surface area and availability of more adsorptive sites. A further increase in catalyst loading to 200g did not result in appreciable increase in the amount of MB adsorbed on the catalyst. Probably, the MB molecules available are not sufficient for adsorption by the increased number of available adsorptive sites. Hence, the additional TiO₂ pellets are not involved in the adsorption process and the rate does not increase with increase in the amount of catalyst.

4.2 Adsorption Isotherms

An adsorption isotherm is used to characterize the equilibria between the amount of adsorbate that accumulates on the adsorbent and the concentration of the dissolved adsorbate. Adsorption isotherms are important for the description of how an adsorbate will interact with an adsorbent and are critical in optimizing the use of an adsorbent [86]. The interactions of MB molecules with the catalyst were validated with the Langmuir and the Freundlich adsorption isotherms. The Langmuir adsorption isotherm is based on a kinetic approach and assumes a uniform surface, a single layer of adsorbed material and a constant temperature. Freundlich isotherm deals with heterogeneous surface adsorption [87], it is an empirical equation based on the distribution of the solute between the solid phase and the aqueous phase at equilibrium.

The Langmuir model is given by the following relation:

$$\frac{Q_e}{Q_m} = \frac{bC_e}{1 + bC_e} \quad (10)$$

The linearized form of the Langmuir model is

$$\frac{C_e}{Q_e} = \frac{1}{bQ_m} + \frac{C_e}{Q_m} \quad (11)$$

where C_e is the liquid-phase concentration of the adsorbate at equilibrium (mg/L), Q_e is the amount of adsorbate adsorbed at equilibrium (mg/g), Q_m is the maximum adsorption capacity (mg/g) and b is the Langmuir constant related to the energy of adsorption (L /mg).

The Freundlich model relationship is as follows:

$$Q_e = K_f C_e^{-n} \quad (12)$$

The linearized Freundlich model relationship is:

$$\ln Q_e = \ln K_f + \frac{1}{n} \ln C_e \quad (13)$$

K_f is a constant indicative of the adsorption capacity of the adsorbent ((mg/g) (L/g)^{1/n}), q_m is the maximum adsorption capacity (mg/g), C_o is the initial adsorbate concentration (mg/L) and n is an empirical constant related to the magnitude of the adsorption driving force according to Halsey [88].

$$K_f = \frac{q_m}{C_o^{1/n}} \quad (14)$$

The adsorption of MB on the TiO₂ pellet can be described by the Freundlich isotherm (figure 4.2) than the Langmuir isotherm model (appendix A5). The applicability of the Freundlich isotherm implies that heterogeneous surface conditions exist under the experimental conditions investigated i.e. the TiO₂ pellets have a distribution of pores with different shapes and sizes [86] rather than monolayer adsorption assumed in Langmuir model.

The Freundlich constants K_f and n were estimated by the linear regression analysis of the experimental adsorption data of MB. For an X-Y plot of Equation (8), where $Y = \ln Q_e$ and $X = \ln C_e$, the slope is $1/n$ and intercept is $\ln K_f$.

$K_f = 4.4287E-07$ and $n = 2.7556$. (Figure 4.2)

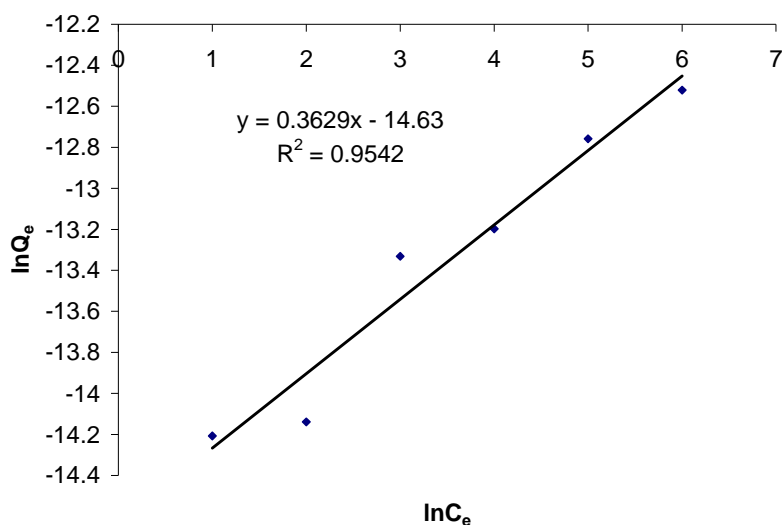


Figure 4.2: Freundlich Plot of MB adsorption onto TiO_2 Pellet.

4.3 Batch Degradation Experiment

A preliminary control experiment was carried out to examine the effect of UV light on MB, by illuminating ($10\mu\text{M}$) methylene blue solution without TiO_2 catalyst. To determine the optimum catalyst loading of the novel photoreactor, separate experiments were then carried out with different loadings of TiO_2 catalyst with UV illumination for the photocatalytic degradation of ($10\mu\text{M}$) MB aqueous suspension.

Figure 4.3 shows the results of the MB control and batch degradation experiments. There was only a slight change noticed in the MB colour with the UV irradiation (control) experiment with approximately 18% reduction in the residual MB concentration. Significant changes in MB colour were observed in the residual solution with the experiments with various loadings of TiO_2 with UV irradiation. The colour changes gradually from blue to a colourless solution at the end of 60 min irradiation.

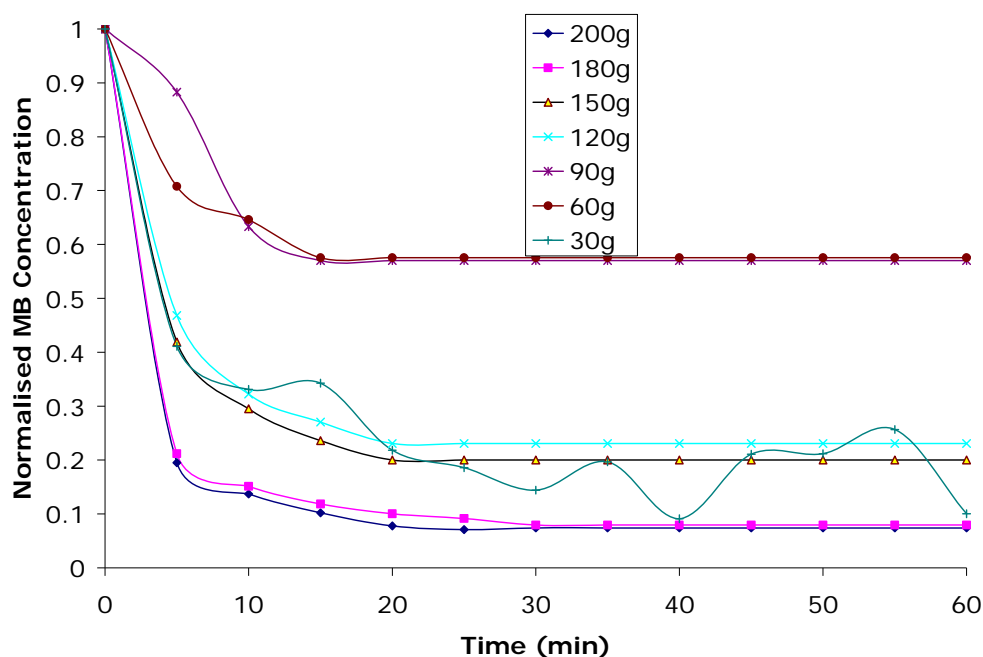


Figure 4.3. Batch degradation of MB at various loadings of TiO₂. C₀=10μM, V=1L.

The rate of photodegradation was studied by monitoring the change in the maximum absorption in UV-visible spectra at 666 nm of the residual MB solution over irradiation time. The disappearance of MB colour observed in the degradation reactions with catalyst loading but without irradiation was due to adsorption of MB molecules onto the catalyst surface rather than photocatalyzed degradation. This conclusion was supported by the observation that, the final solution from the photocatalyzed degradation experiments was clearer and colourless compared to the slightly blue coloured residual solution of the non-irradiated set [84], indicating that the presence of TiO₂ played an important role in the photodegradation of MB.

Approximately 99% reduction in residual MB concentration of was observed within 30 min of irradiation for the 200g catalyst loading; 98% for 180g, 90% for 150g, 98% for 120g, 94% for 90g loading, 93% for 60g and only 69% reduction was observed for the lowest catalyst loading of 30g for 30 min irradiation. However, at the end of 60 min irradiation, 97% reduction was achieved with 30 g catalyst loading.

Assuming that the hydroxyl radical OH^\bullet is the primary oxidant for the degradation of MB [103], a chemical kinetics for the process may be written as:



The rate of degradation of MB can be expressed as:

$$r = \frac{dC}{dt} = \frac{kKC}{1 + KC} \quad (16)$$

Where r is the rate of degradation of reactant (mg/L min), C concentration of the reactant (mg/L), t the illumination time (min), k the reaction rate constant (min^{-1}) and K is the adsorption coefficient of the reactant (L/mg). When the reactant concentration is micromolar, equation (12) can be simplified to an apparent first-order equation.

$$\ln\left(\frac{C_o}{C}\right) = kKt = K_{app} \quad (17)$$

A plot of $\ln(C_o/C)$ against time represents approximately linear straight lines, showing the case of the first-order reaction. The slope of the line equals the apparent first-order rate constant K_{app} .

The experimental data from the degradation of MB on 30, 60 and 90 g loadings of TiO_2 fitted well with the first-order reaction kinetics (Figure 4.4 for 60g TiO_2 loading) compared to the zero-order reaction kinetics (appendix Fig. A6), while the TiO_2 loadings on 200, 180, 150 and 120 g do not follow a particular order. The determined K_{app} values are summarised in table 3.0

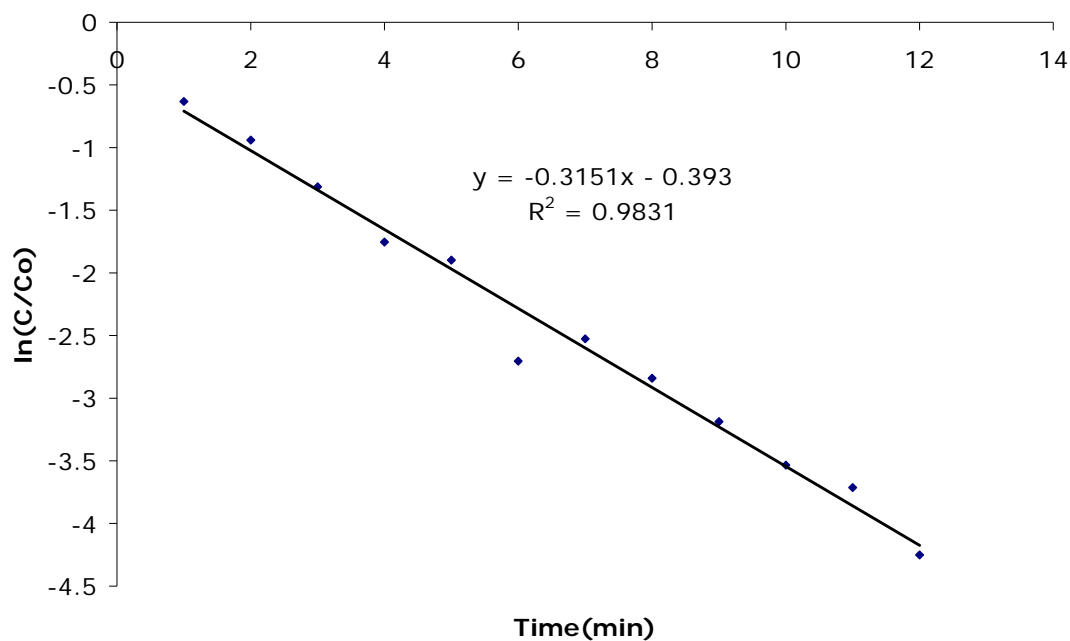


Figure 4.4: First-order-reaction kinetics of MB degradation on 60g TiO₂ loadings.
C₀ = 10μM.

Catalyst Weight(g)	Rate constant (min ⁻¹)	r ²	Q _e (mg/g)
200	0.3266	0.6769	4.22E-08
180	0.1729	0.6208	4.67E-08
150	0.2750	0.7918	4.32E-08
120	0.2593	0.7202	5.15E-08
90	0.3044	0.9196	2.41E-08
60	0.3151	0.9831	4.49E-08
30	0.2597	0.9588	-6.10E-08
UV Alone	0.0191	0.7802	

Table 3: Summary kinetic data of MB batch degradation on TiO₂ catalyst.
C₀=10μM, V=1L, irradiation time = 60mins.

The results show that the rate of degradation of MB on TiO₂ catalyst increased initially as the catalyst loading was increased from 30 g/L to 60 g/L. Further increase in TiO₂ loading from 60 g/L to 180 g/L shows a reduction in the rate of degradation,

except for 200g that showed the highest rate, apparently due to an increase in the amount of photons absorbed by the TiO₂ catalyst. The observed increase in degradation rate as catalysts loading was increased from 30 g/L to 60 g/L can be explained by the fact that there was an increased in the photon adsorption with increased loading. Further increase from 60 g/L to 180 g/L resulted in decreased degradation rate, except for 200 g/L catalyst loading that shows an exceptional increased rate.

However, the highest catalyst loading of 200g does not exhibit a corresponding highest equilibrium adsorption of MB, apparently due to insufficient number of MB molecules available for adsorption onto the additional number of TiO₂ sites available. Although the density of TiO₂ pellets in the area of illumination increases, at the prevalent initial concentration of MB, the number of MB molecules in solution stays the same. The additional catalyst pellets are not involved in the photocatalysed process.

A similar result was reported by Sivalingam et al., [89] in the photocatalytic degradation of various dyes by combustion synthesized nano anatase TiO₂ in a jacketed quartz tube photoreactor. The initial rate of degradation was reported to reached saturation for catalyst loading (P-25) above 1kg/m³ for MB concentration of (25-200) ppm. In slurry photocatalytic processes, catalyst dosage is an important parameter that has been extensively studied [2, 13, 47, 68, 90]. Optimum catalyst dosage reported in literature varied from 0.15 to 8 g/L for different photocatalyzed system and photoreactors. Even for the same catalyst (Degussa P25), a big difference in optimal catalyst dosage (from 0.15 to 2.5 g/L) was reported. No general conclusion has been made to date [2].

The lower catalyst loading of 30 g/L shows (Figure 4.5) a modest degradation rate with approximately 97% MB degradation achieved at the end of 60 min UV irradiation. Only approximately 18% degradation was observed with the control experiment (UV alone).

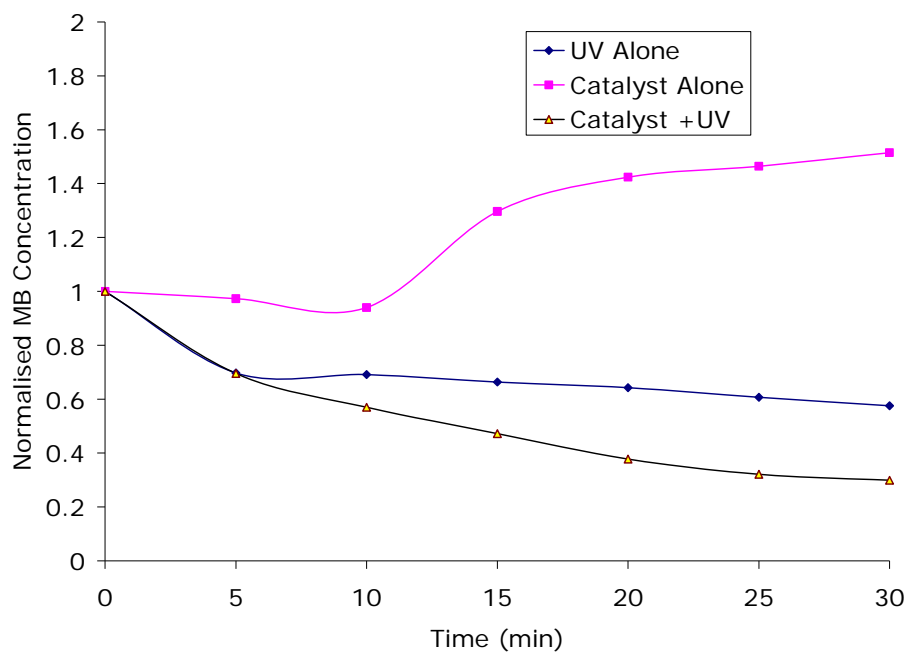


Figure 4.5: Rate of Change in MB degradation with irradiation with 30g Catalyst loading. $C_0=10\mu\text{M}$, $V=1\text{L}$.

The batch experimental data of 30g TiO_2 loading fitted well with the first-order reaction kinetics (Figure 4.6).

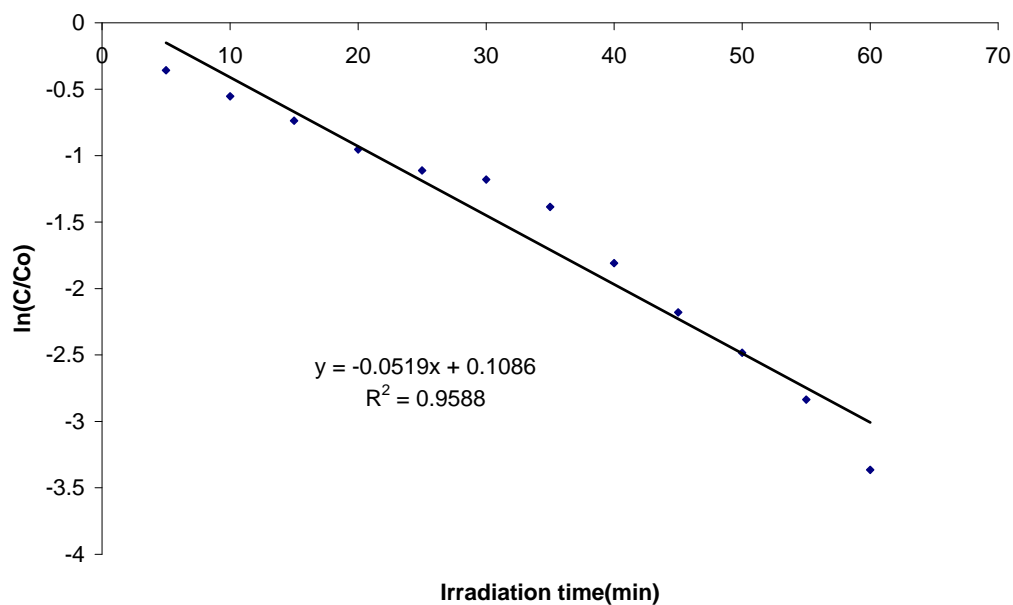


Figure 4.6: First-order-reaction kinetics of Methylene blue degradation on 30g/L load of TiO_2 pellet.

The higher TiO₂ loadings though gave a faster degradation rate, but they also facilitated TiO₂ disintegration as more pellets are available for collusion during the agitation of the reaction vessels which resulted in pulverization of the TiO₂ pellets. The lower catalyst loading of 30 g/L was therefore chosen for subsequent experiments.

4.4 Methylene Blue TOC analysis.

The degradation rate for the mineralization and decomposition of MB is shown in figure 4.7. Approximately 78% reduction in TOC was observed at the end of 60 min irradiation. The reduction in TOC after degradation confirms the mineralization efficiency of the novel photocatalytic reactor.

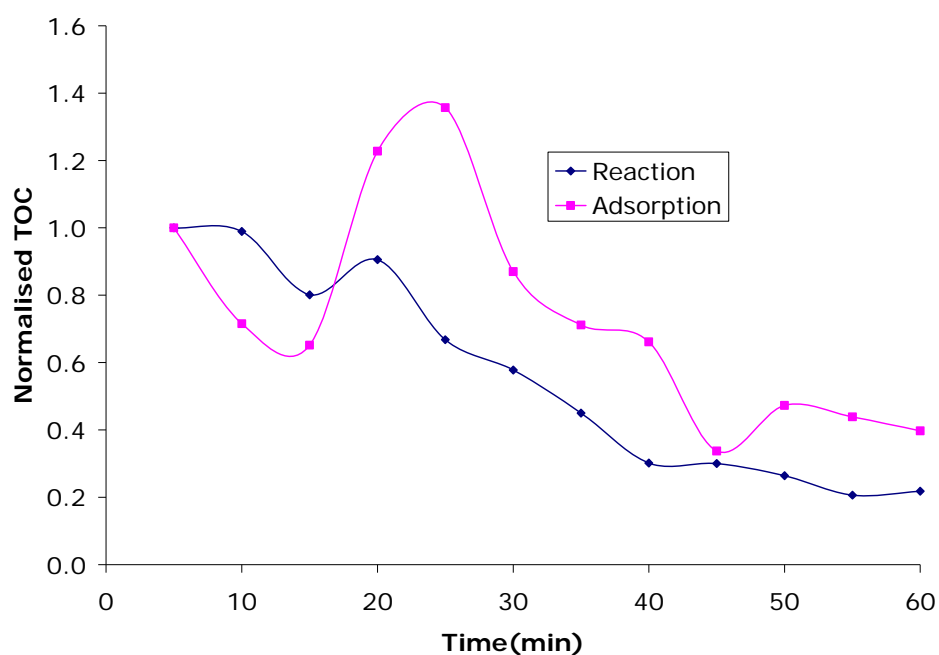


Figure 4.7: Depletion in TOC of MB batch mineralization with 30 g/L loading. C₀ = 10μM.

4.5 Continuous Flow MB Degradation.

In any design for industrial waste treatment application, high wastewater throughput in the reactor must be attainable [74]. A Batch reactor, although efficient in photodegradation, is limited in reactor throughput i.e. only small volumes of water can be treated at any given time. Batch reactors are difficult to scale up, continuous flow reactors configuration are well suited for industrial application [78]. They provide for the continuous operation of the photocatalytic reactor and are easy to scale up, once the mass transfer characteristics of the catalyst and the reaction kinetics parameters have been evaluated.

4.5.1 Effect of Number of Reaction vessel

Figures 4.8. shows the results of the MB adsorption on TiO_2 in a continuous flow pattern with recirculation of the aqueous suspension of MB with 1, 2, and 3 reaction vessels connected in series. The result show that approximately 68 % adsorption was achieved with a single vessel ($C_o = 10\mu\text{M}$, $V=1\text{L}$, $W= 30 \text{ g}$), 63 % ($C_o= 10\mu\text{M}$, $V=2\text{L}$, $W= 60 \text{ g}$) with two vessels connected in series and 72 % for the three reaction vessels connected in series ($C_o= 10\mu\text{M}$, $V = 2\text{L}$, $W= 90 \text{ g}$)

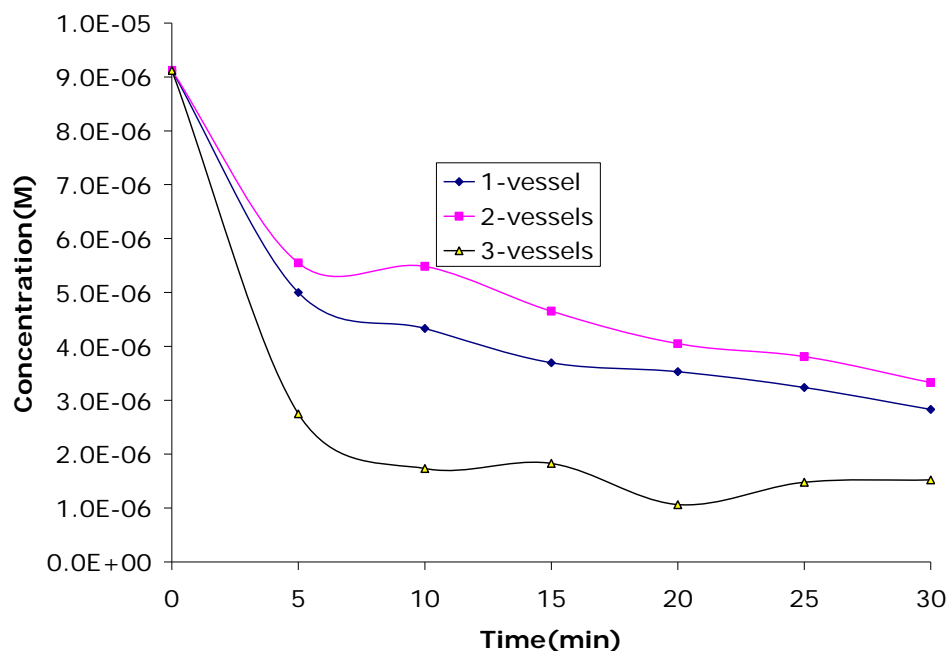


Figure 4.8: Continuous flow MB Adsorption on 30 g/L TiO_2 loading, $C_o = 10\mu\text{M}$.

Figure 4.9. shows the result of the photocatalytic degradation of MB with one reaction vessel in a continuous flow pattern. The results shows no significant degradation with UV irradiation alone (18% reduction), compared with 86% degradation of MB observed at the end of 60 min irradiation. The degradation result indicated that the MB degradation was higher in the batch experiment (98%) than flow with continuous recirculation experiments, under same initial MB concentration and catalyst loading ($C_0 = 10\mu\text{M}$, $W = 30\text{ g/L}$).

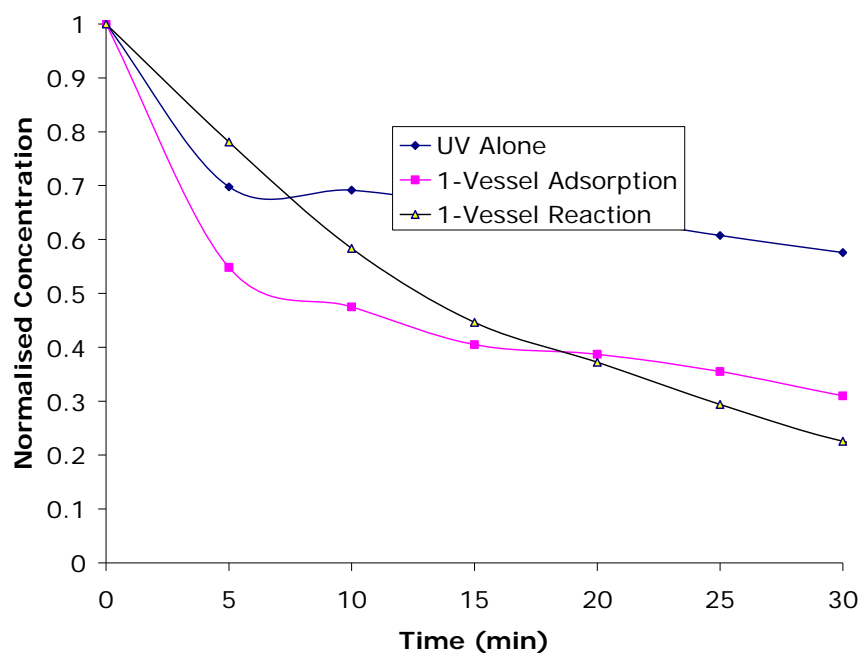


Figure 4.9: Continuous flow MB degradation (1-reaction vessel) $C_0 = 10\mu\text{M}$, $V = 1\text{L}$, recirculation flow rate = 2.7 ml/s.

Figure 4.10. show the results of the MB degradation in a continuous flow pattern with recirculation of the aqueous suspension of MB with two reaction vessels. The result of the experiment shows that 84% degradation was achieved with the two reaction vessels connection in series at the end of 60 min irradiation.

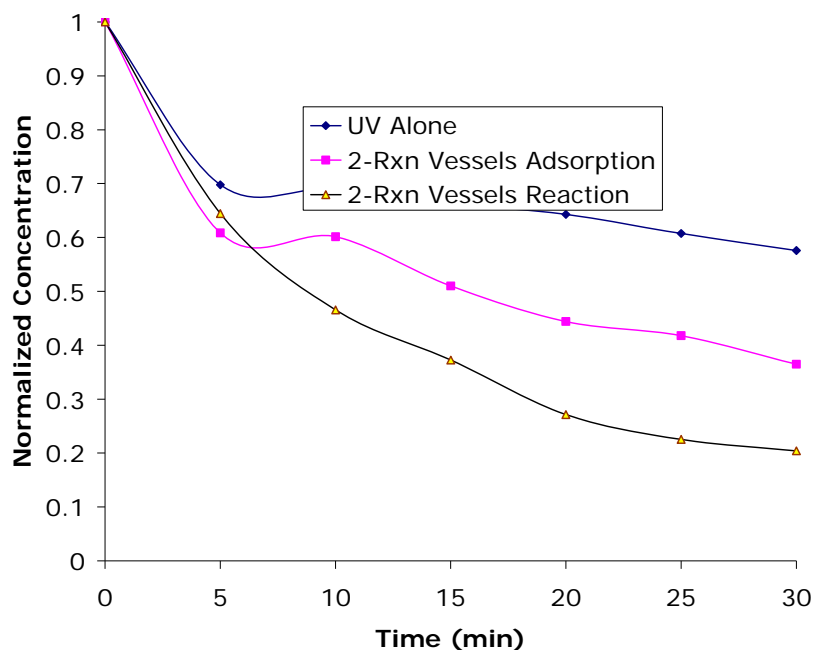


Figure 4.10: Continuous flow MB degradation (2-reaction vessels)

$C_0 = 10\mu\text{M}$, $V = 2\text{L}$, recirculation flow rate = 2.7ml/s , TiO_2 loadings = 60g .

Figure 4.11. shows the results of the continuous flow degradation of MB with three reaction vessels connected in series with recirculation. 89% degradation was achieved at the end of 60 min irradiation of 2 Litres of ($10\mu\text{M}$) MB aqueous suspension with 90g of TiO_2 .

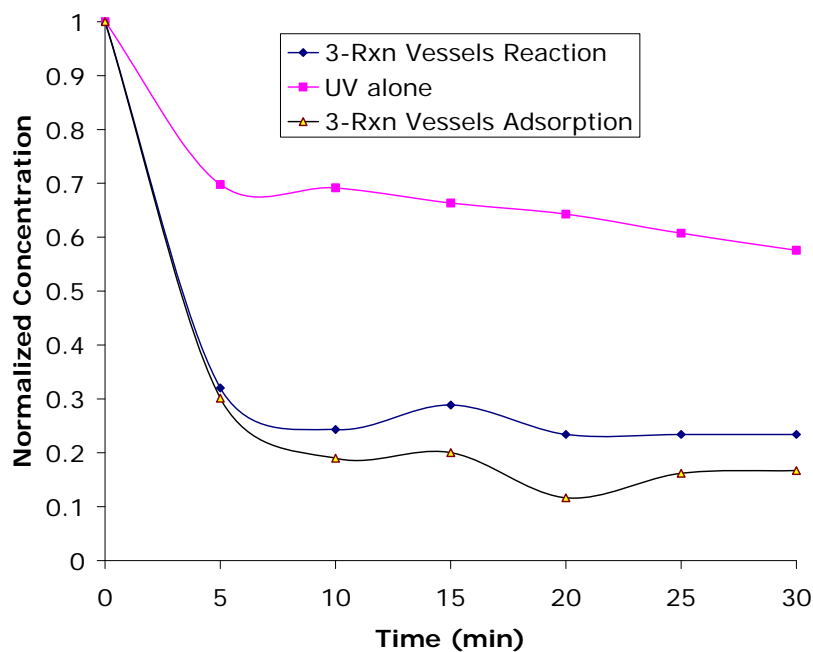


Figure 4.11: Continuous flow MB degradation (3-reaction vessels).

$C_0 = 10\mu\text{M}$, $V = 2\text{L}$, recirculation flow rate = 2.7ml/s , TiO_2 loading = 90g .

Figure 4.12 compares the degradation of MB achieved with one, two and three reaction vessels operating in a continuous flow mode under experimental conditions; $C_0=10\mu\text{M}$, recirculation rate = 2.7 ml/s, TiO_2 loadings = 30g (1- vessel), 60 g (2- vessels) and 90 g (3-vessels).

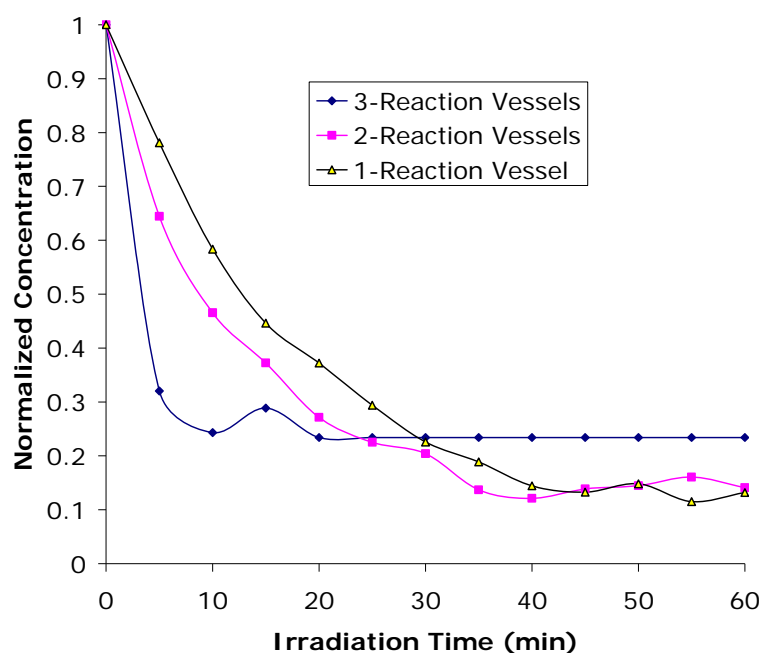


Figure 4.12: Continuous Flow MB degradation with 1, 2, and 3 Vessels.

Table 4 summarises the first-order reaction rate constants for the continuous flow MB degradation. As can be seen from the results, the single reaction vessel shows a higher degradation rate. This can be attributed to the short time it takes to get the aqueous suspension back to the illumination zone, as the number of photon absorbed influences the rate of generation of the hydroxyl radical necessary for photodegradation.

	First-order-reaction rate constant (min^{-1})	r^2	Catalyst loadings (g)
1-Vessel	0.1678	0.9237	30
2-Vessels	0.1233	0.7826	60
3-Vessels	0.139	0.8300	90

Table 4: MB continuous flow reaction rate constants.

Comparing the result of the batch MB degradation with the continuous flow result under similar experimental conditions ($C_0 = 10\mu\text{M}$, $V = 1\text{L}$, recirculation flow rate = 2.7ml/s , TiO_2 loading = 30g) shows (Figure 4.13) that the batch degradation was faster than the continuous flow with recirculation, confirming the resident time effect on degradation rate.

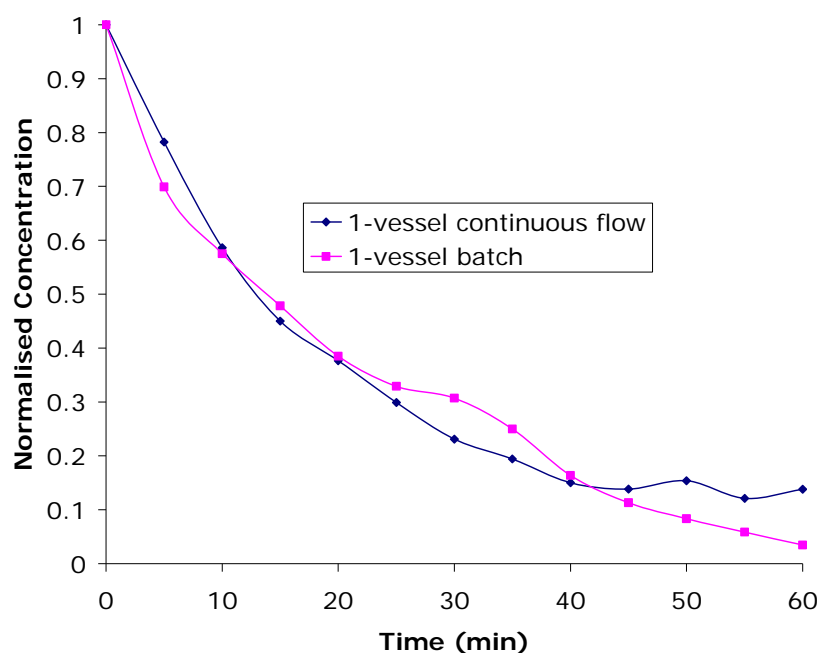


Figure 4.13: Comparison batch vs. continuous flow MB degradation. $C_0 = 10\mu\text{M}$, $V = 1\text{L}$, recirculation flow rate = 2.7ml/s , TiO_2 loading = 30g .

Yamazaki et al., [91] reported a similar reduction in degradation rate in their continuous flow experiment than results obtained in the batch experiment, in the photocatalytic degradation of trichloroethylene (TCE) solution in a recirculation system through a packed bed reactor with TiO_2 pellets. They concluded that only a small portion of the circulated suspension was illuminated. The degradation rate in circulated system was reported to decrease by ca 20% for P-25[91].

4.5.2 Effect of Recirculation rate on MB degradation.

Changes in the speed of rotation of the reaction vessels will not only cause more turbulent flow in the reaction vessels, but it will also affect the recirculation rate of the aqueous suspension between the reactor and the reservoir.

The results of the effect of changes in the rate of recirculation of the continuous flow experiment for methylene blue degradation with one vessel with recirculation is shown in figure 4.14. The results show that the rate of degradation reduces as the recirculation rate is increased. Apparently due to shorter contact time of aqueous suspension with illumination source as increased recirculation rate, as a result of increased speed of rotation of the reaction vessels will result in more liquid getting expelled from the reaction vessel.

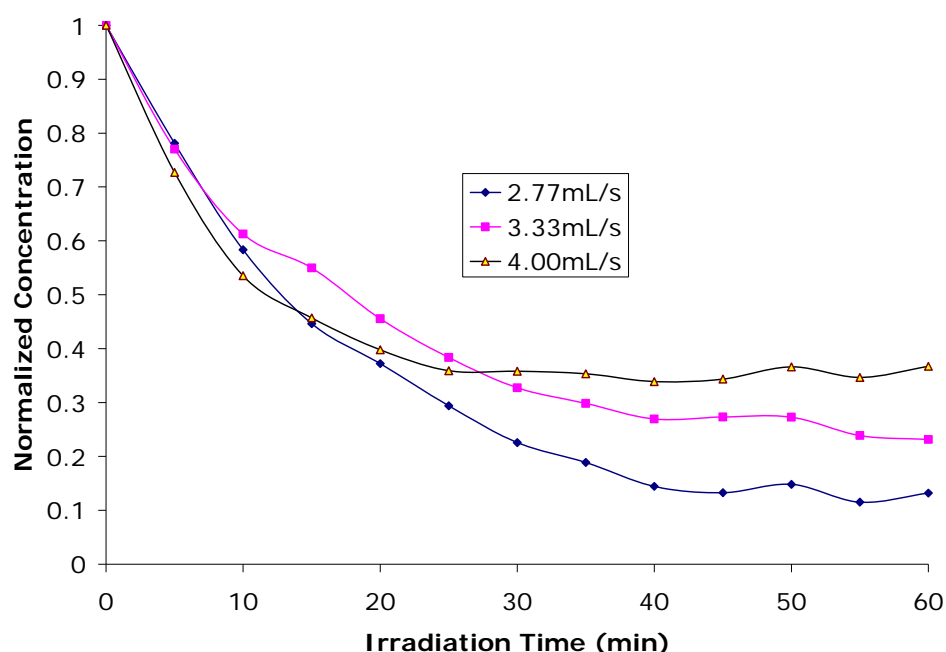


Figure 4.14: Effect of recirculation rate on MB degradation.

$C_o = 10\mu\text{M}$, TiO_2 loading = 30g, $V = 1 \text{ L}$ (1-vessel).

Table 5 summarises the first-order reaction rate constant for the low and medium recirculation rate. While the high recirculation rate (4.00mL/s) degradation did not follow a particular order. (See appendix A15 and A16 for both first and zero order linear plots). The lowest recirculation rate showed the highest reaction rate. Catalyst disintegration was observed more at the higher speed of rotation. Therefore, to avoid

the need of separation of pulverized pellets in treated solution, most of the tests were performed at 2.77 ml/s.

Recirculation rate	First-order reaction rate constant (min ⁻¹)	r ²
2.77ml/sec	0.0345	0.9254
3.33ml/sec	0.0212	0.9213
4.0ml/sec	0.0097	0.5769

Table 5: MB continuous flow reaction rate constants (speed of rotation).

Most of the reported studies in the photodegradation of organic compounds in aqueous medium using TiO₂ as photocatalyst have been carried out using fine particle TiO₂ in suspension. In such slurry photoreactor, higher circulation flow rate was reported desirable to ensure uniform dispersion of TiO₂ aggregates, avoid mass transfer limitation and to overcome the problem of dissolved oxygen depletion [92].

4.6 Congo red dye (CR) degradation.

Azo dyes contains one or more azo bond (-N=N-) and they account for more than 60 to 70% of all dyestuffs used in the textile industry [93]. Other functional group characterizing these class of compounds are also the auxochromes such as -NH₂, -OH, -COOH, -SO₃H which are responsible for the increase of colour intensity and the affinity with the fibers [94]. Congo red is a recalcitrant azo dye found in textile wastewater [95]. It is a direct dye and classified as an anionic dye. The important substituents in the dye structure are the two sodium sulphonate groups, -SO₃Na, each of which attaches to one of the two naphthalene rings and makes congo red highly soluble in water [95, 96] therefore, their removal from wastewater is difficult. In an aqueous solution, congo red ionizes into two sodium cations and two coloured sulphonate anions [95, 96].

The rate of decomposition of (10 μ M) congo red dye solution with TiO₂ catalyst (30 g) under UV irradiation for 60 min is shown in figure 4.15. The result shows that congo red dye seems not to be amenable to photocatalytic degradation under UV illumination. Only approximately 32% degradation was achieved within 60 min irradiation and just about 10% adsorption was achieved on TiO₂. No appreciable change was observed with the UV irradiation (control) experiment.

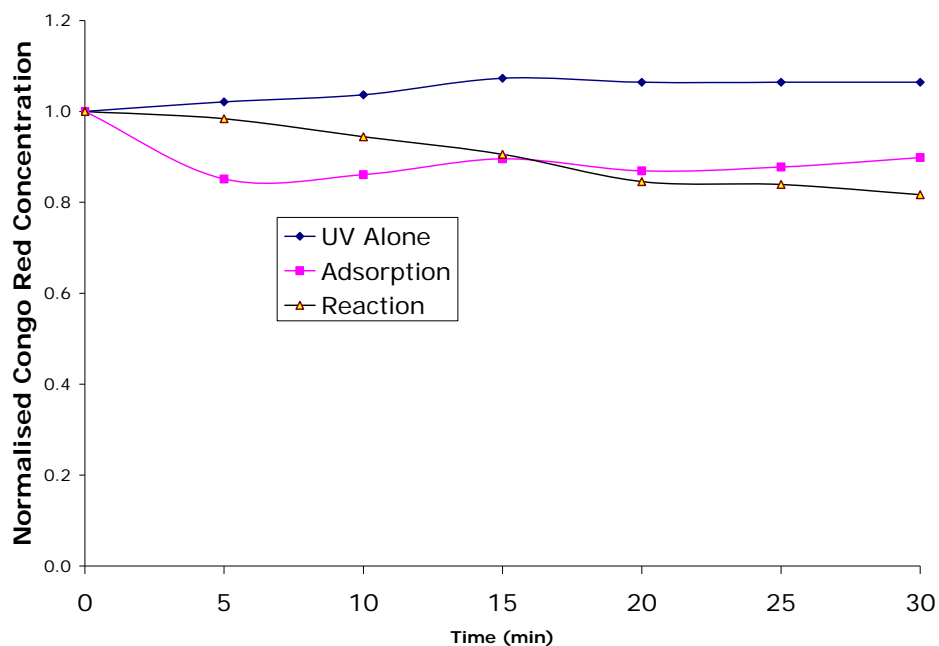


Figure 4.15: Congo red continuous flow photocatalytic degradation. $C_0=10\mu\text{M}$, TiO₂ = 30g, irradiation time = 60 min.

Figure 4.16 illustrates the TOC results for congo red mineralization using continuous flow photocatalysis. The mineralization (depletion of TOC content vs. irradiation time) results also reaffirmed the low degradation of congo red dye. Approximately 30% reduction in TOC was observed.

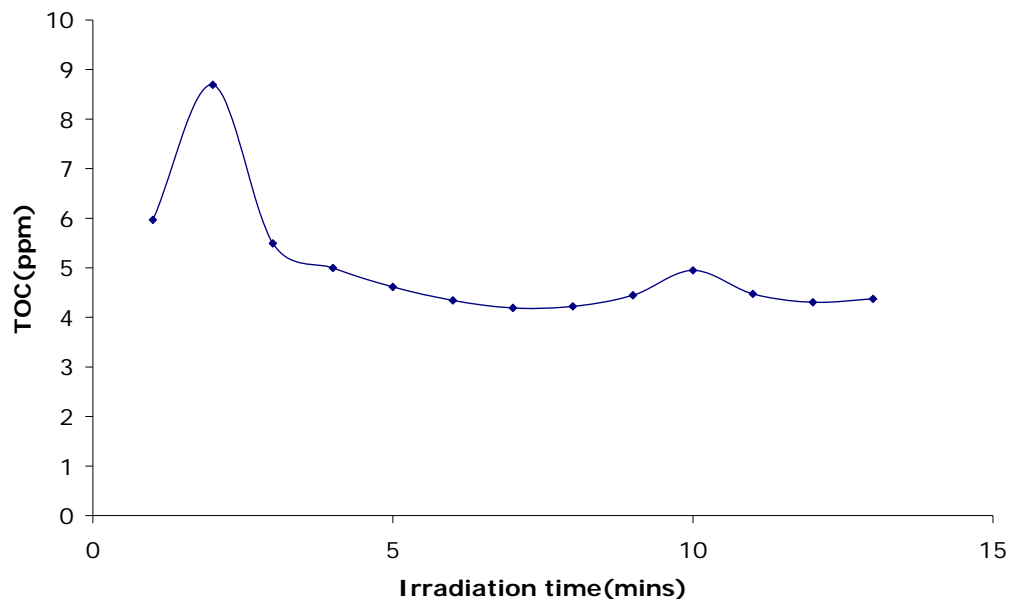


Figure 4.16: Congo red mineralization (TOC).

Guillard et al., [97] reported similar low degradation rate of congo red dye with a cascade falling film photoreactor with titania supported on non-woven inorganic fibers. Steric hindrance of the large aromatic molecule in the congo dye structure which leads to a small number of CR molecule been adsorbed on TiO_2 was reported responsible for the low degradation rate.

4.7 Acridine Orange Degradation.

Acridine orange (AO) is a heterocyclic dye containing nitrogen atoms which is widely used in the field of printing and dyeing, leather, printing ink and lithography [98]; the dye is also used extensively in biological staining [99]. It is a serious pollutant in wastewater and difficult to treat by common removal methods such as coagulation and biodegradation [98].

The results of acridine orange experiments are shown in figure 4.17. Under alkaline conditions, the TiO_2 surface is reported to carry a weak negative charge, while AO is primarily positively charged, which facilitates adsorption and promote photocatalytic degradation [98]. The result of AO the adsorption (95 %) on TiO_2 (appendix A10) and the rate of degradation (figure 4.17) support the observation of Chung-Shin et al., [98].

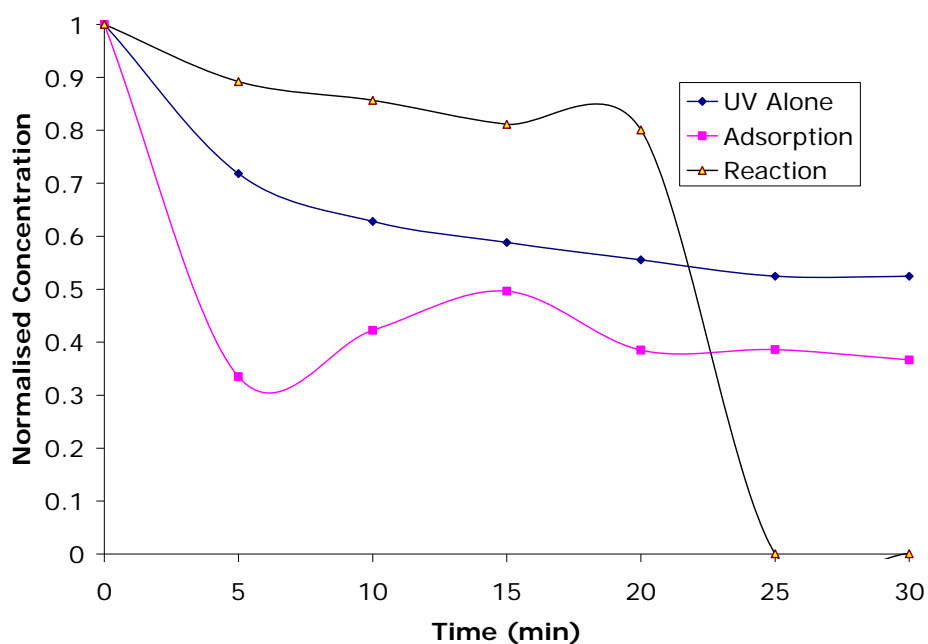


Figure 4.17: Acridine Orange photocatalytic degradation. $C_0=100\mu\text{M}$, $\text{TiO}_2 = 30\text{g}$, irradiation time = 60min.

Figure 4.18 shows the TOC analysis of acridine orange mineralization. The TOC value was observed to increased with increasing irradiation time, probably due to evaporation.

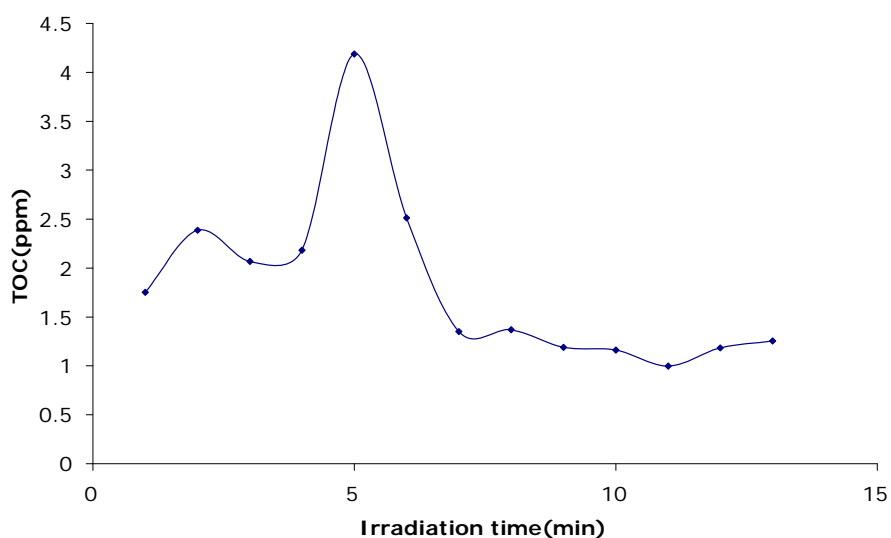


Figure 4.18: Acridine Orange mineralization, $C_0= 100\mu\text{M}$, $\text{TiO}_2= 30 \text{ g/L}$.

5.0 Produced Water mineralization

The temporal depletion of TOC in the photocatalytic degradation of produced water sample under UV irradiation for 60 min is shown in Figure 4.19. The result showed that approximately 78% reduction in TOC was achieved at the end of 60 min of UV irradiation.

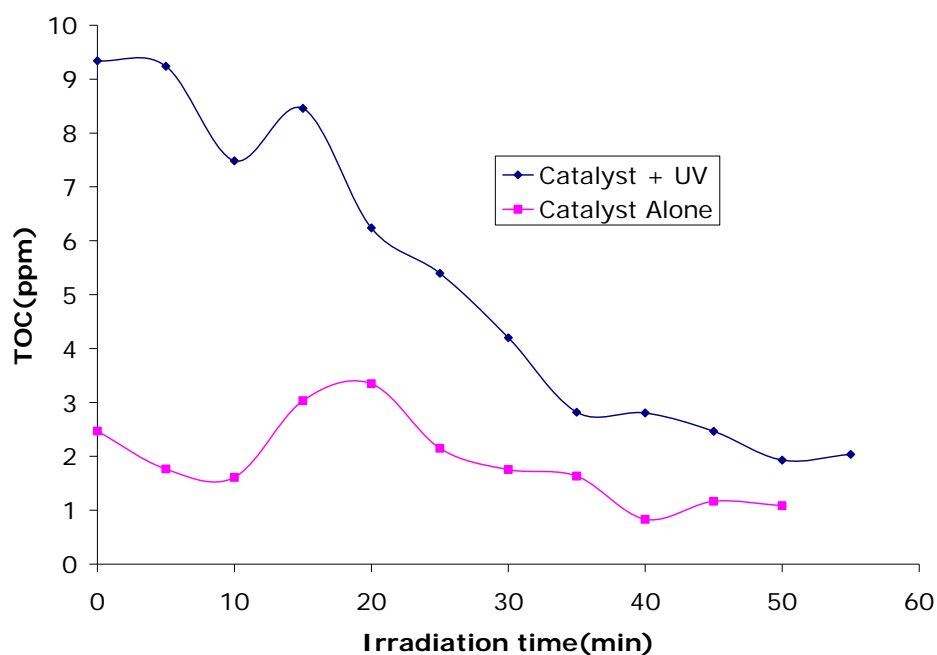


Figure 4.19: sample produced water mineralization (TOC).TiO₂=30g.

The kinetics of the TOC elimination fitted well with the first-order-reaction kinetic (Figure 4.20). (See appendix A17 for zero order kinetics)

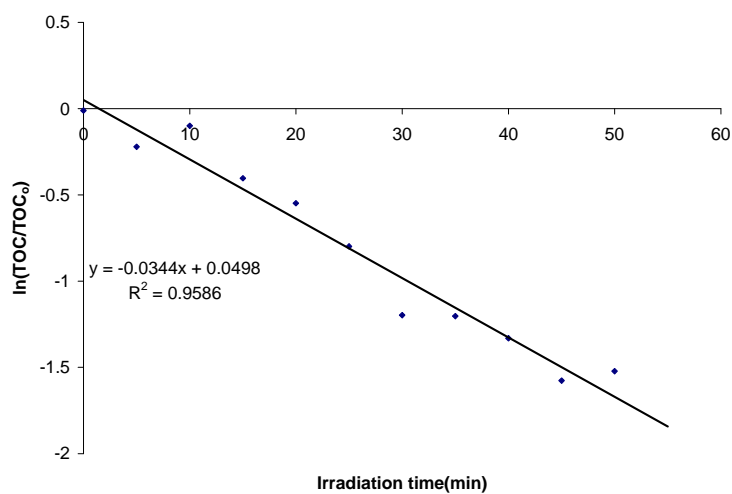


Figure 4.20: First-order-reaction kinetic of produced water demineralization (TOC)
 $TiO_2=30\text{g/L}$, irradiation time = 60min.

Water Quality Parameter	Parameter Concentration
pH	6.8 – 7.2
Dissolved Oxygen (mg/L)	Less than 0.1
Total Dissolved Solids (TDS) (mg/L)	49,971
Total Nitrogen (mg/L)	34
Total Phosphorus (mg/L)	9.21
Chloride (mg/L)	25,502
Calcium (mg/L)	2,668.9
Magnesium (mg/L)	369.1
Sodium (mg/L)	12,878
Sulphate (mg/L)	621.3
TPH (mg/L)	64
TNA (mg/L)	62
Heavy Metals (mg/L)	
Arsenic	0.05
Barium	0.25
Cadmium	0.006
Chromium	0.01
Lead	0.08
Mercury	0.002
Selenium	0.05
Silver	0.02

Table 6: Water Chemistry analysis of oilfield produced water collected from a Roswell, New Mexico surface pit [100].

The extent of decomposition from a comparison of UV absorbance of the produced water could not be analyzed because the composition of the real produced water sample is unknown. Typical produced water effluent composition is shown in table 6. The quality of produced water generated varies depending on the method of recovery and the nature of the formation. Many hydrocarbon compounds present in produced

water have become solubilized during their subsurface coexistence with either crude oil or natural gas [100]. Produced water retains similar organic compound characteristics present in their oil/gas counterpart. Composition consists mainly of n-alkanes C_{10} and larger hydrocarbons. Typical total n-alkane (TNA) concentration range from 1 to 200 mg/L. When in solution, volatilization or physical stripping of these organic are fairly limited due to their low vapor pressures. In general, the produced waters that accumulate in pits (open system) are typically non-volatile hydrocarbon. [100].

However, the TOC reduction achieved with the UV illumination of this real sample of produced water indicated that TiO_2 mediated photocatalysis could be successfully applied to remove the hydrocarbon component of produced water discharge from oil rig waste water.

6.0 Photocatalytic Degradation with Degussa P-25 TiO_2

Degussa P-25 TiO_2 is one the most widely applied commercial catalyst in photocatalysis research and has been used in many research to analyse the photocatalytic efficiency of different reactors. In order to compare the efficiency of the novel reactor, P-25 TiO_2 catalyst batch experiment was carried out.

The result of MB degradation ($10\mu M$) with degussa P-25 TiO_2 powder (0.1 g/L) (BET surface area $\sim 50\text{m}^2\text{ g}^{-1}$) under similar experimental condition as the pellets TiO_2 catalyst shows (Figure 4.21) a much shorter degradation time of less than 10min for the complete degradation of a $10\mu M$ aqueous solution of MB and a first-order reaction kinetics ($k = 0.0744\text{ min}^{-1}$) (Figure 4.22).

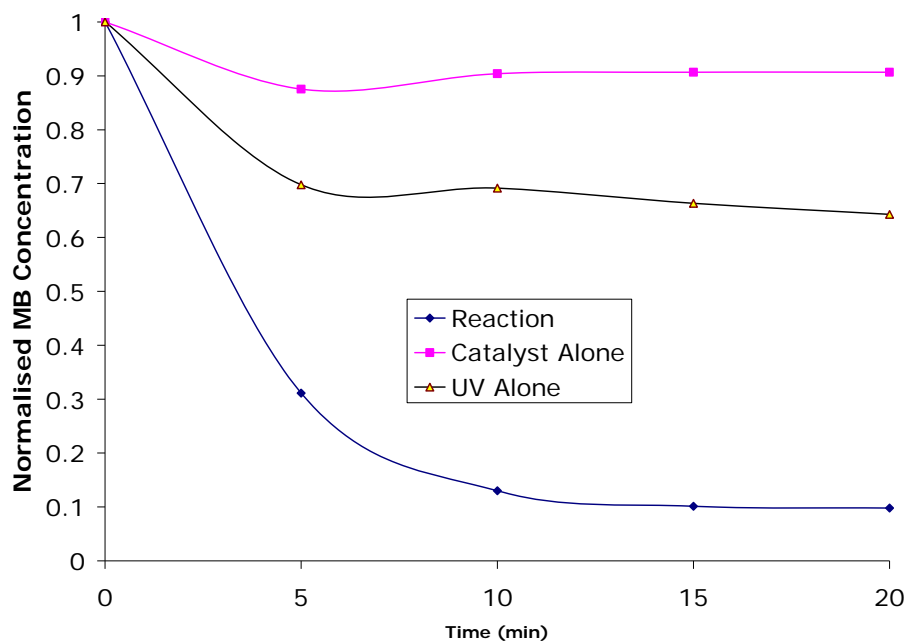


Figure 4.21: Change in concentration of MB with irradiation time on P-25 TiO₂ catalyzed photodegradation, (C₀=10μM), (P-25=0.100g).

Apparently, the novel reactor configuration exposes a large number of the catalyst particle to the illumination zone. Resulting in the generation of more hydroxyl radicals to drive the MB degradation process.

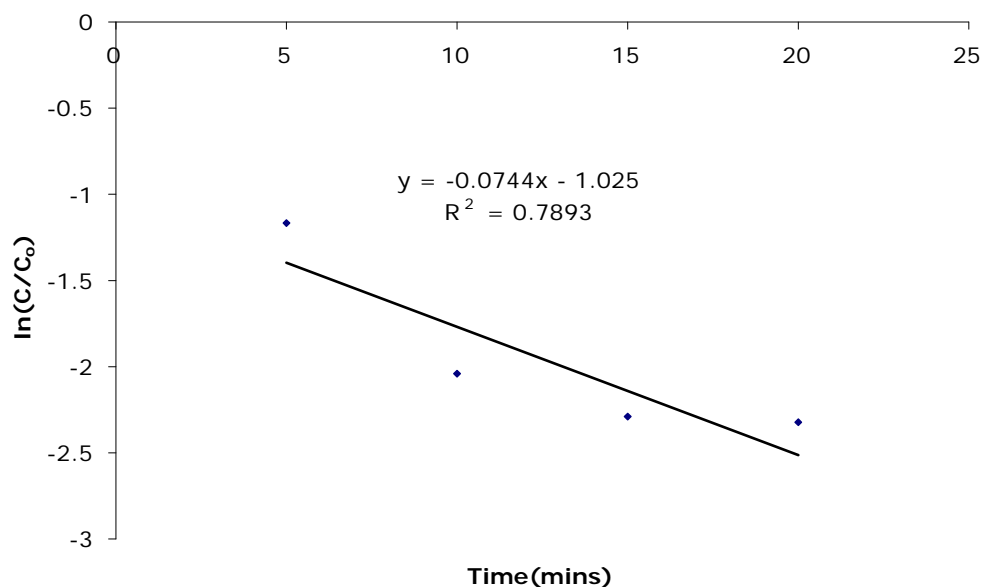


Figure 4.22: First-order-reaction kinetics linear plot of Methylene blue degradation on P-25 Degussa TiO₂ powder = 0.1 g/L, C₀ = 10μM.

The result of the P-25 comparison experiment of approximately 98% degradation of MB aqueous suspension under UV irradiation within 10 min compared well with results reported in literature: 34 min for 70% degradation reported by Lakshim et al.,[101], 120 min for 100% degradation reported by Zhang et al.,[24], 270 min for 100% degradation reported by Otsuka-Yao and Ueda [102], 20 min for 80% degradation by Mozia et al.,[58], 120 min for 100% degradation by Naska et al.,[100]. The result of the P-25 MB degradation is not a direct comparison of the novel reactor performance with the reactors used in literature, it is just to compare the performance with trends reported in literature since the operational parameters of the various reactor defers.

CHAPTER 5

CONCLUSIONS AND FUTURE WORK

5.0 Conclusion

In this work, a novel slurry-continuous-flow reactor, employing a commercial pellet TiO₂ catalyst, was evaluated. The novel reactor was tested for its ability to degrade a range of organic pollutants (methylene blue, congo red, acridine orange) and sample produced water. The experiments were conducted with relatively small initial concentrations of reactant typically found in industrial waste water discharges. No attempt was made to adjust the pH of the solution; experiments were carried out in natural pH and at room temperature for both dark adsorption and photocatalytic degradation. Adsorption and degradation were monitored with UV-Visible spectrophotometry and TOC analysis.

The novel photoreactor was investigated in terms of four operational parameters; (1) TiO₂ loading, (2) flow rate, (3) batch vs. continuous flow pattern, and (4) number of reaction vessels. Methylene blue dye was used to optimize the TiO₂ loading of the reactor with respect to the rate of adsorption and photocatalytic degradation under UV illumination in the batch experiment. Commercially available Hombikat KOC pellet TiO₂ catalyst was used in this novel photoreactor.

In this work, the rate of adsorption of methylene blue dye on the pellet catalyst was investigated, and the results of the equilibrium adsorption data was validated with both Freundlich and Langmuir model to determine its adsorption isotherm. The result fitted well with the Freundlich model, indicating that under the experimental condition, the adsorption of MB on the pellet is a heterogeneous surface adsorption.

The effect of catalyst loadings on the rate of adsorption was also investigated. The results shows that the rate of adsorption initially increased as the catalyst loadings was increased until an optimum load of 180g under experimental conditions ($C_0=10\mu\text{M}$,

V=1L, rate of recirculation =2.77ml/s) where a further increase to 200g did not result in corresponding increase in MB adsorption.

The rate of MB degradation with various loads of catalyst was also investigated in batch experiments. It was found that the rate of degradation increased with increased catalyst loading from 30g to 180g, until an optimum loading was reached and further loading did not result in an appreciable increase in degradation rate of MB. A modest loading of 30g /L TiO₂ was chosen for further experiments based on the result (97 % reduction within 60min of irradiation time) of the batch experiment. The experimental data of Methylene blue degradation fitted well with the first-order reaction kinetics, while produced water TOC reduction also fitted well with the first-order reaction kinetics.

The effect of operating the novel reactor in a continuous flow pattern with one, two, and the third reaction vessel in series on MB degradation was investigated and the results showed an increase in MB degradation rate with the three reaction vessels connected in series. The higher degradation results from the continuous flow experiment with the three reaction vessels connected in series, coupled with the use of pellet TiO₂ makes the novel reactor design likely to be useful in large scale application as it eliminates the need for separation of catalyst particle after degradation process associated with slurry reactor. The TiO₂ pellets are porous; therefore, they provide a large surface area for the adsorption and subsequent degradation of organic pollutant in water.

The effect of recirculation rate as a result of change in speed of rotation of the reaction vessels experiments results showed that higher speed is not desirable as the time the aqueous suspension is exposure to illumination is reduced and catalyst disintegration due to collision of pellets against the paddle increases. This results in blockage of fluid passages.

In order to compare the performance of the novel reactor with other reactor designs reported in literature using commercial P-25 TiO₂, a batch experiment for MB

degradation using P-25 TiO₂ was investigated. The result of the comparison experiment of P-25 TiO₂ showed that the novel reactor configuration allows a good mixing of pollutant with catalyst, the formation of the thin liquid film allowed efficient exposure of both catalyst and solution to light irradiation, and the aqueous suspension was well dispersed in the illumination zone. Other model organic contaminants (acridine orange and produced water sample) were successfully degraded with the novel photocatalytic reactor, while congo red dye was partially degraded.

5.1 Future Work

The effect of light intensity was not investigated in this work; further investigative work on the novel photoreactor should include an analysis of the effect of irradiation intensity on the reactor performance. Also, alternative light transmitting material could be investigated for the construction of the reaction vessel (e.g. borosilicate glass) cylinders. Solar irradiation could also be investigated with the novel reactor configuration.

The effect of pH on degradation rate was not investigated in this work; further work should include this, as literature reviews have established that pH variation has direct impact on the photocatalytic degradation rate [13, 89].

The catalyst regeneration capability was not investigated in this work; further study could establish the strength of the pellet catalyst for long usage and regeneration capability. Intermediate products of photocatalytic degradation was not identified at this level of investigation, further study could highlighted the intermediate product as well as pollutants degradation pathways.

One of the problems that arise from the reactor operation is the pulverization of the pellets TiO₂, as a result of the attrition action of the rotation of the reaction vessels. First, a means of removing the fine particles from the process fluid either in the reservoir or the confinement of the fine particles inside the reaction vessels should be investigated. Or the replacement of the paddle constructed inside the reaction vessels with a softer material to reduce pellet pulverization, as fine particles blocks connecting tubes and disrupts the flow of fluids within the reactor set up.

CHAPTER 6

REFERENCES

- [1] H, Al-Ekabi; N, Serpone. *Journal of Physical Chemistry* 92 (1988) 5726.
- [2] D, Chen; A.K. Ray. *Applied Catalysis B: Environmental* 23 (1999) 143.
- [3] C. M, Ling; A.R, Mohammed; S, Bhatia. *Chemosphere* 57 (2004) 547.
- [4] O, Zahraa; L, Sauvanaud; G, Hamard; M, Bouchy. *International Journal of Photoenergy* 05 (2003) 87.
- [5] D, Gregory. *Journal of Society of Petroleum Engineers, SPE* 86800 (2004) 15.
- [6] M, Jacob; E, Olliveros; O, Legrini; A.M. Braun (Eds.). *TiO₂ photocatalytic Treatment of Water, Reactor Design and Optimization Experiments. In Photocatalytic Purification and Treatment of Water and Air.* D,F. Ollis; H, Al-Ekabi ed., Elsevier Science Publishers BV, Amsterdam, The Netherlands, 1993.
- [7] B, Knudsen; L, Hjelsvold; M, T.K, Svarstad; M.B.E, Grini; P.G, Willumsen; H, Torvik. *Journal of Society of Petroleum Engineers, SPE* 86671(2004) 1.
- [8] M, Hoffmann. *Chemical Review* (1995) 69.
- [9] U, Periyathamby; A, K. Ray. *Journal of Chemical Engineering Technology*, 22 (10) (1999) 881.
- [10] Ralph, W. Matthews. *Water Research*, 20 (1986) 569.

- [11] K, Gerard. Environmental Engineering, International Edition, McGraw Hill, (1996) 319.
- [12] Ganesh, R; G, D. Boadman; D, Michelson. Water Research, 28 (1994) 1367.
- [13] H, Lachheb; E, Puzenat; A, Houas; M, Ksibi; E, Elaloui; C, Guillard;J, Herrmann. Applied Catalysis B: Environmental 39 (2002) 75.
- [14] H, Zollinger. Colour Chemistry; Synthesis, Properties and Application of Organic Dyes and Pigments, VCH Publishers, New York. (1983) 589.
- [15] A, Fernandez; G, Lassaletta; V, M. Jimenez; A, Justo; A, R. Gonzalez-Elipe; J, Herrmann; H, Tahiri; Y, Ait-Ichou. Applied Catalysis B: Environmental 7 (1995) 49.
- [16] S, Preety; A, K. Ajay. Chemical Engineering Technology 22 (1999) 3.
- [17] B, W. Atkinson; F, Bux; H, C. Kasan. Water, Air, and Soil Pollution 24 (1998) 2.
- [18] K, M. Bansal. Journal of Society of Petroleum Engineers, SPE 46576 (1998) 7.
- [19] G, F. Bennett. Critical Reviews in Environmental Science and Technology 18 (1988) 189.
- [20] A, K. Ray. Catalysis Today 40 (1998) 73.
- [21] A, M. Braun; M, T. Maurette; E, Oliveiros. Photochemical Technology, John Wiley and Sons, Chichester, England, 1993.
- [22] T, Zhang; T,K. Oyama; S, Horikoshi; H, Hidaka; J, Zhao; N. Serpone. Solar Energy Materials and Solar Cells 73 (2002) 287.

- [23] N, Serpone; E, Pellizzetti (Eds.). Photocatalysis; Fundamental and Application, Wiley, New York, 1989.
- [24] D, F. Ollis. Photocatalytic Purification and Treatment of Water and Air, Elsevier, Amsterdam, 1993.
- [25] C, S. Turchi; D, F. Ollis. Journal of Catalysis 122 (1990) 178.
- [26] R, Venkatadri; R, Peter. Hazardous Waste Hazardous Matter 10 (1986) 107.
- [27] H, Ted; W, Nan-min; Z, Faqin. Water Research 34 (2000) 407.
- [28] M, R. Samarghandi; J, Nouri; A, R. Mesdaghinia; A, H. Mahvi; S, Nasser; F, Vaezi. International Journal of Environmental Science and Technology. 4 (2007) 19.
- [29] D, L. Sedlak; A, W. Andren. Environmental Science and Technology 25 (1991) 777.
- [30] R, W. Matthews. Pure and Applied Chemistry 64 (1992) 1285.
- [31] A, L. Pruden; D, F. Ollis. Journal of Catalysis 82 (1983) 404.
- [32] I, Poulios; I, Tsachpinis. Journal of Chemical Technology and Biotechnology 74 (1999) 349.
- [33] X, Qi; Z, Wang; Y, Zhuang; Y, Yu; J, Li. Journal of Hazardous Materials 118 (2005) 219.
- [34] N, Rao; S, Dube. Indian Journal of Chemical Technology 4 (1997) 6.
- [35] M, Sökmen; D, W. Allen; F, Akkaş; N, Kartal; F, Acar. Water, Air, and Soil Pollution 132 (2001) 153.

- [36] C, Shifu. *Environmental Science and Technology* 17 (1996) 33.
- [37] N, Subrata; P, Arumugom; C, Manas. *Journal of Photochemistry and Photobiology A: Chemistry* 113 (1998) 257.
- [38] F, Sunada; A, Heller. *Environmental Science and Technology* 32 (1998) 282.
- [39] N, Takeda; T, Torimoto; S, Sampath; S, Kuwabata; H, Yoneyyama. *Journal of Physical Chemistry; B* 99 (1995) 9986.
- [40] N, Takeda; N, Iwata; T, Torimoto; H, Yoneyyyama. *Journal of Catalysis* 177 (1998) 240.
- [41] K, Tanaka; K, Padermpole; T, Hisanaga. *Water Research* 34 (2000) 327.
- [42] R, W. Matthews. *Journal of Chemical Society Faraday Trans.* 80 (1984) 457.
- [43] R, W. Matthews. *Journal of Physical Chemistry; B* 91 (1986) 569.
- [44] R, W. Matthews. *Journal of Physical Chemistry* 91 (1987) 3328.
- [45] R, W. Matthews. *Journal of Catalysis* 111 (1988) 264.
- [46] A, K. Ray; A, A.C.M. Beenackers. *Journal of American Institute of Chemical Engineers* 44 (1998) 477.
- [47] V, Augugliaro; M, J. López-MuñozL; Palmisano, J. Soria. *Applied Catalysis, B: Environmental* 101 (1993) 7.
- [48] L, Chen; T, Chou. *Industrial Engineering Chemical Research* 32 (1993) 1520.
- [49] J, D'Oliveira; G, Al-Sayyed; P, Pichat. *Environmental Science and Technology* 24 (1990) 990.

- [50] Y, Inel; A, N. Okte. *Journal of Photochemistry and Photobiology A: Chemistry* 96 (1996) 175.
- [51] E, Pellizzetti; N, Serpone (Eds.). *Photodegradation of Organic pollutants in aquatic system catalysed by semiconductors in*; Academic Publishers., Boston, 1988.
- [52] C, Kormann; D, W. Bahnemann; M, Hoffmann. *Environmental Science Technology* 25 (1991) 494.
- [53] D, F. Ollis; C, Y, Hsiao; L, Budiman; C, L. Lee. *Journal of Catalysis* 88 (1984) 89.
- [54] Y, Yu; J,C. Yu; C, Chan; Y, Che; J, Zhao; L, Ding; W, Ge; P, Wong. *Applied Catalysis B: Environmental* 61 (2005) 11.
- [55] C, Bauer; P, Jacques; A, Kalt. *Journal of Photochemistry and Photobiology A: Chemistry* 140 (2001) 81.
- [56] C, Hu; Y, Wang. *Chemosphere* 39 (1999) 2107.
- [57] S, Mozia; M, Toyoda; M, Inagaki; B, Tryba; A, W. Morawski. *Journal of Hazardous Materials* 140 (2007) 369.
- [58] D, F. Ollis; E, Pellizzetti; N, Serpone. *Environmental Science and Technology* 25 (1991) 1523.
- [59] A, E. Cassano; C, A. Martin; R, J. Brandi; O, M. Alfano. *Industrial Engineering Chemical Research* 34 (1995) 2155.
- [60] O, Legrini; E, Oliveros; A, M. Braun, *Chemical Review* 93 (1993) 671.

- [61] T, Oyama; A, Aoshima; S, Horikoshi; H, Hidaka; J, Zhao; N, Serpone. Solar Energy 77 (2004) 525.
- [62] A, Sclafani; A, .R. Brucato. (Eds.). Mass transfer limitations in a packed bed Photoreactor used for phenol removal. In photocatalytic purification and Treatment of Water and Air.1993.
- [63] J, K. Szczechowski; C, Koval; R, D. Noble. Chemical Engineering Science 50 (1995) 3163.
- [64] A, Haartrick; O, M. Kut; E, Heinzle. Environmental Science and Technology 30 (1990) 817
- [65] D, F. Ollis; E, Pellizzetti; N, Serpone (Eds.). Heterogeneous Photocatalysis in the Environment; application to water purification, Wiley, New York., 1989.
- [66] N, J. Peill; M, R. Hoffmann. Environmental Science and Technology 29 (1995) 2974.
- [67] H, C. Yatmaz; C, R. Howarth; C, Wallis. (Eds.). Photocatalysis of organic effluent in a falling film reactor, Elsevier Science Publishers, Amsterdam, The Netherlands, 1993.
- [68] D, D. Dionysiou; G, Balasubramanian; M, T. Suidan; A, P. Khodadoust; I, Baudin; J, Laine. Water Research 34 (2000) 2927.
- [69] D, Bockelmann; R, Goslich; D, A.B. Weichgrete. (Eds.). Solar detoxification of polluted water; comparing the efficiency of a parabolic through reactor and a novel thin film-fixed-bed reactor, Elsevier Science Publishers BV., Amsterdam, The Netherlands., 1993.

- [70] A, K. Ray; A, A.C.M. Beenackers, (1996). European Patent 96200942.9-2104.
- [71] L, Rideh; A, Wehrer; D, Ronze; A, Zoulalian. *Industrial Engineering Chemical Research* 36 (1997) 4712.
- [72] M, F.J. Dijkstra; A, Michorius, H. Buwalda, H.J. Panneman, J.G.M. Winkelman and A.A.C.M. Beenackers, *Catalysis Today* 66 (2001) 487.
- [73] K, Mehrotra; G, S. Yablonsky; A, K. Ray. *Industrial Engineering Chemical Research* 42 (2003) 2273.
- [74] H, F. Lin; R, Ravikrishna; K.T. Kalliat. *Separation and Purification Technology* 28 (2002) 87.
- [75] H, F. Lin; K, T. Valsaraj. *Journal of Hazardous Materials* (2003) 203.
- [76] N, Maya; L, Zhenghao; H, Adam. *Industrial Engineering Chemical Research* 32 (1993) 2318.
- [77] K, K. Ioannis; T, Konstantinou; A, A. Triantafyllos. *Applied Catalysis B: Environmental* 49 (2004) 14.
- [78] T, Zhang; T, Oyama; S, Horikoshi; J, Zhao; H, Hidaka; N, Serpone. *Solar Energy* 71, 5, (2001) 305.
- [79] L, M. Hitchman; T, Fang. *Journal of Electroanalytical Chemistry*. (2002) 539.
- [80] H, T. Chang; N, Wu; F, Zhu. *Water Research* 34 (2000) 407.
- [81] L, Palmisano; A, Scalfani. *Heterogeneous Photocatalysis*, John Wiley & Sons, Chichester, UK, 1997.

- [82] R, W. Matthews. *Water Research* 20 (1998) 569.
- [83] Perspex product Data Summary, www.perspex.co.uk
- [84] S, Naskar; S, Arumugom Pillay; M, Chanda. *Journal of Photochemistry and Photobiology A: Chemistry* 113 (1998) 257.
- [85] I, K. Konstantinou; T, A. Albanis. *Applied Catalysis B: Environ* 49 (2004) 14.
- [86] O, Hamdaoui. *Journal of Hazardous Materials* 135 (2006) 264.
- [87] C, H. Giles; T,H. MacEwam; S,N. Nakhwa; D, Smith, *Journal of Chemical Society* 10 (1960) 3973.
- [88] G, D. Halsey. *Advanced Catalysis*. 4 (1952) 269.
- [89] G, Silvalingam; K, Nagaveni; M, S. Hegde; M, Giridhar. *Applied Catalysis, B: Environmental* 45 (2003) 23.
- [90] C, H. Hung; B, J. Marinas. *Environmental Science Technology* 31 (1997) 562.
- [91] S, Yamazaki; S, Matsunaga; K, Hori. *Water Research* 35 (2001) 1022.
- [92] G, Sagawe; R, J. Brandi; D, Bahnemann; A, E. Cassano. *Solar Energy* 77 (2004) 471.
- [93] M, Muruganandham; M, Swaminathan. *Solar Energy Materials and Solar Cells* 81 (2004) 439.
- [94] R, Molinari; F, Pirillo; M, Falco; V, Loddo; L, Palmisano. *Chemical Engineering and Processing* 43 (2004) 1103.

- [95] K,W. Rajeev; W,Y. Williams; L, Yunping; I,M. Michelle; C,F. Joshua; N, Whitney; L,C. Vicki . Journal of Molecular Catalysis A: Chemical 242 (2005) 48.
- [96] F, Yuzhu; T, Viraraghan. Bioresource Technology 82 (2002) 139.
- [97] C, Guillard; H, Lachheb; A, Houas; M, Ksibi; E, Elaloui; J, Herrmann. Journal of Photochemistry and Photobiology A: Chemistry 158 (2003) 27.
- [98] C, Lu; F, Mai; C, Wu; R, Wu; C, Chen. Dyes and Pigments 20(2007) 1.
- [99] M, Faisal; M, Abu Tariq; M, Muneer. Dyes and Pigments 72 (2007) 233.
- [100] T, T. Gilbert; N, Nirmalakhandan; I, G. Jorge. Water Research 29 (1995) 1711.
- [101] S, Lakshmi. Journal of Photochemistry and Photobiology A: Chemistry 88 (1995) 163.
- [102] S, Otsuka-Yao-Matsuo; M, Ueda. Journal of Photochemistry and Photobiology A: Chemistry 168 (2004) 6.
- [103] M. M, Mohammed; M.M, Al-Esaimi. Journal of Molecular Catalysis A: Chemical 255(2006) 53.

CHAPTER 7

APPENDIX

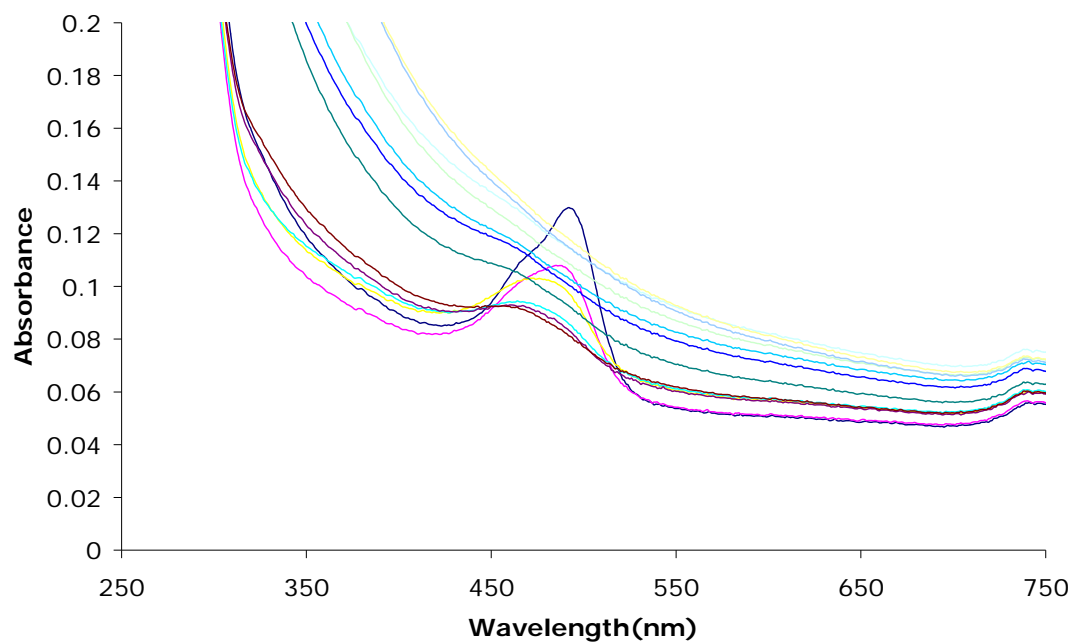


Figure A1: Acridine orange Absorption Spectra over (250-750) nm wavelength. maximum absorbance at 495nm.

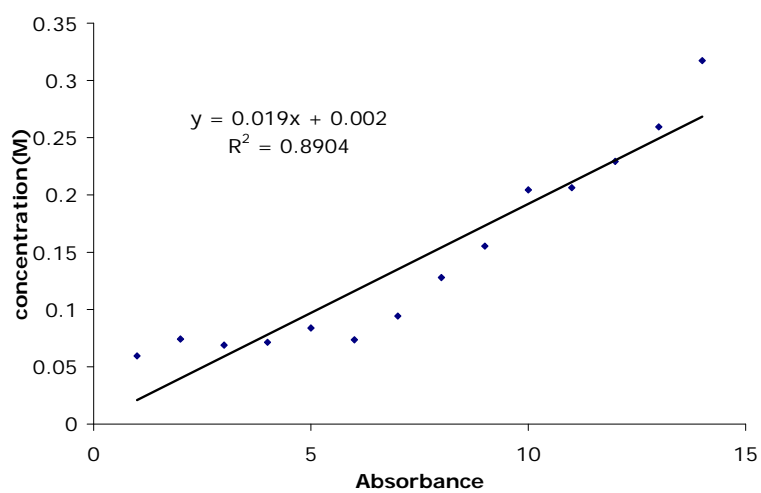


Figure A2: Acridine Orange Calibration Plot.

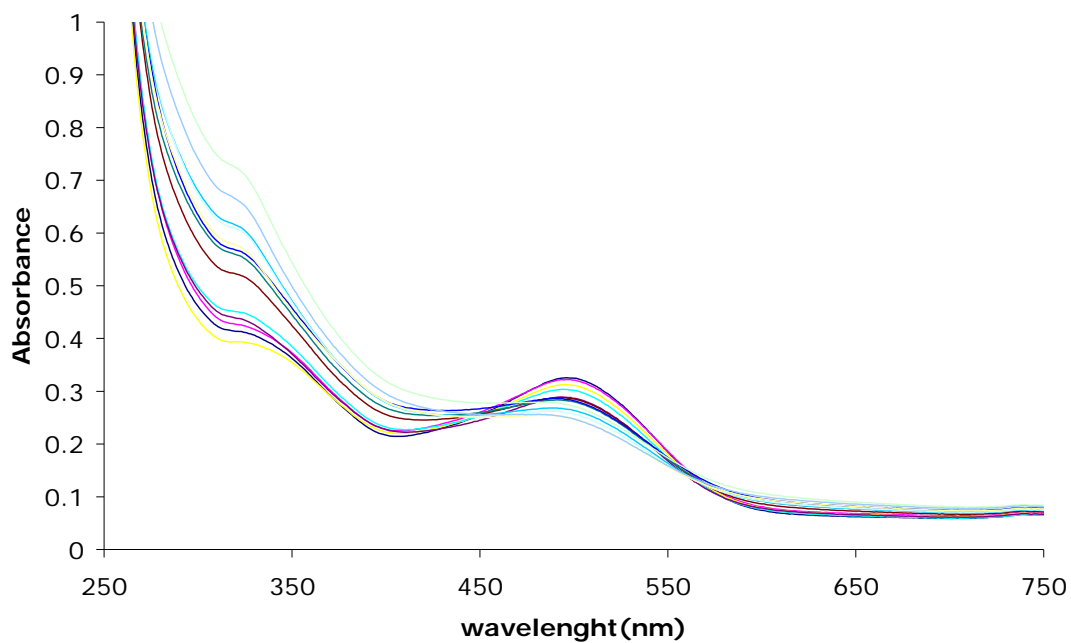


Figure A3: congo red Absorbance spectra over (250-750) nm wavelength and maximum absorbance at 503nm.

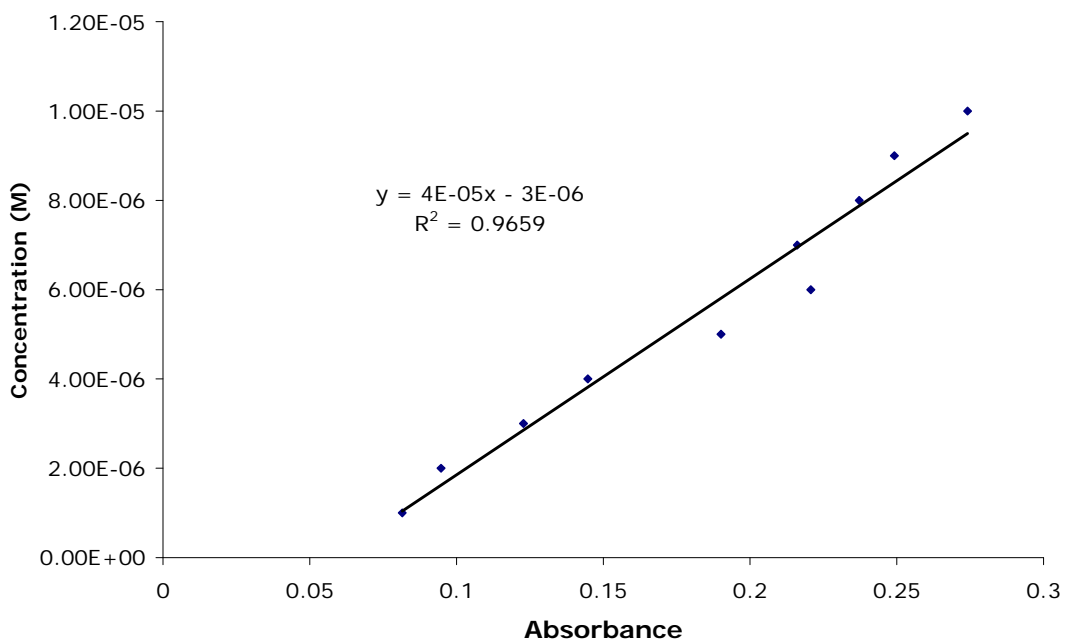


Figure A4: Congo red Calibration Plot.

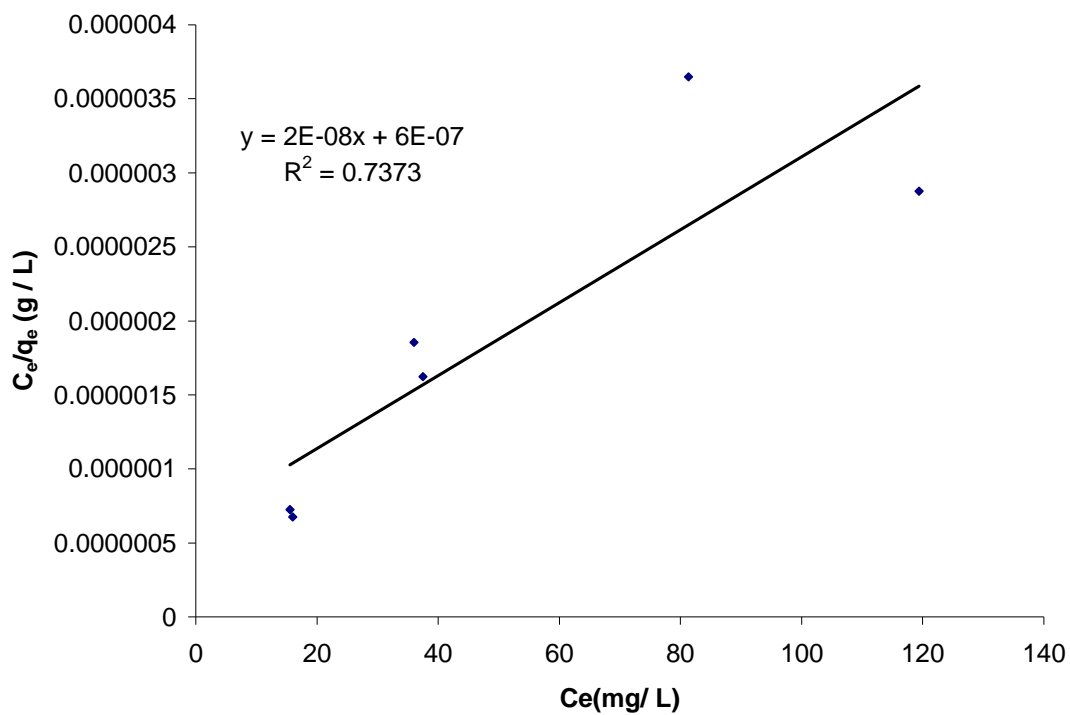


Figure A5: Langmuir Plot of MB adsorption onto TiO_2 Pellet.

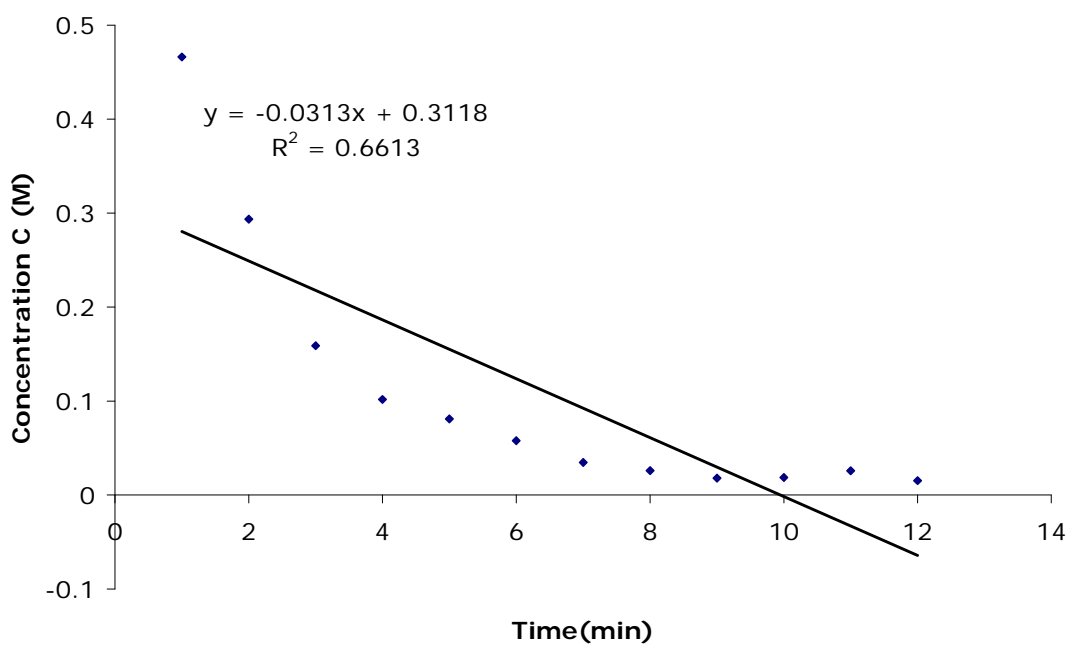
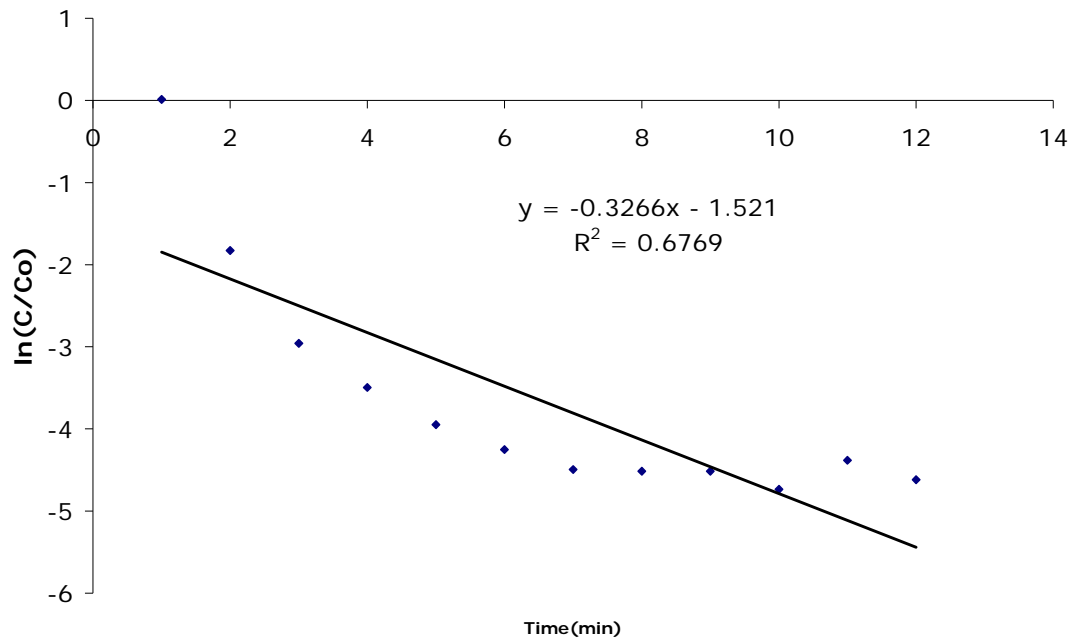
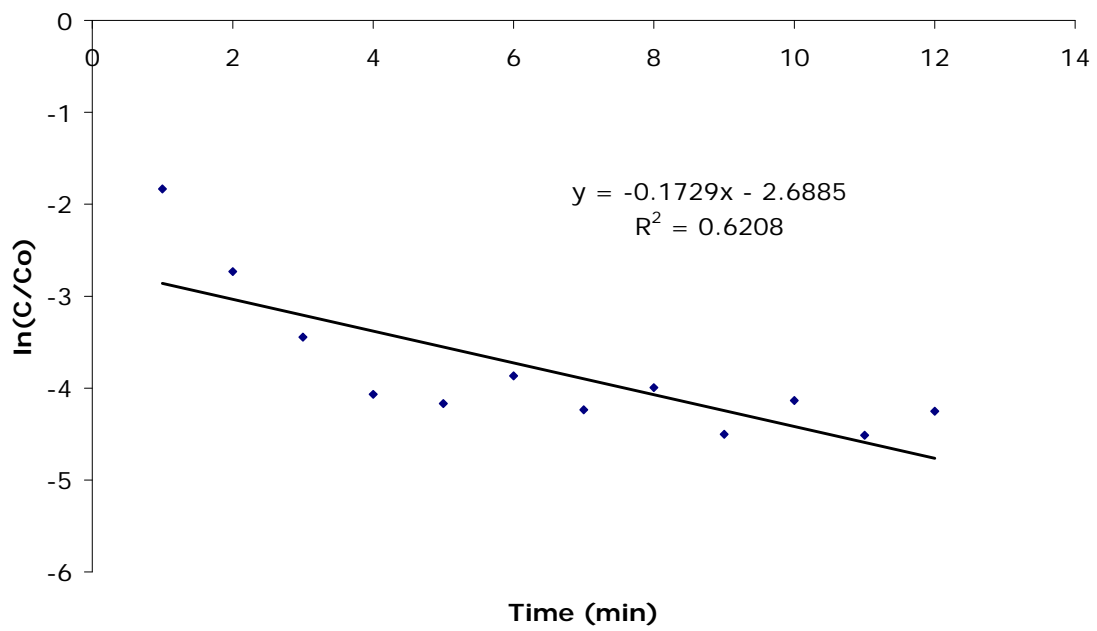


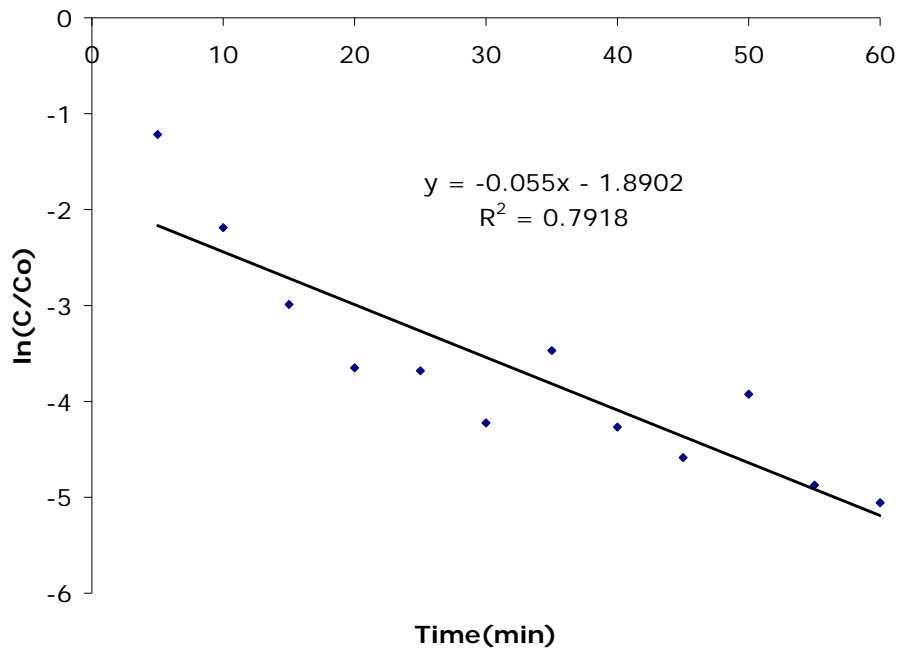
Figure A6: Zero-order-reaction-kinetics of MB degradation on 90g TiO_2 loading



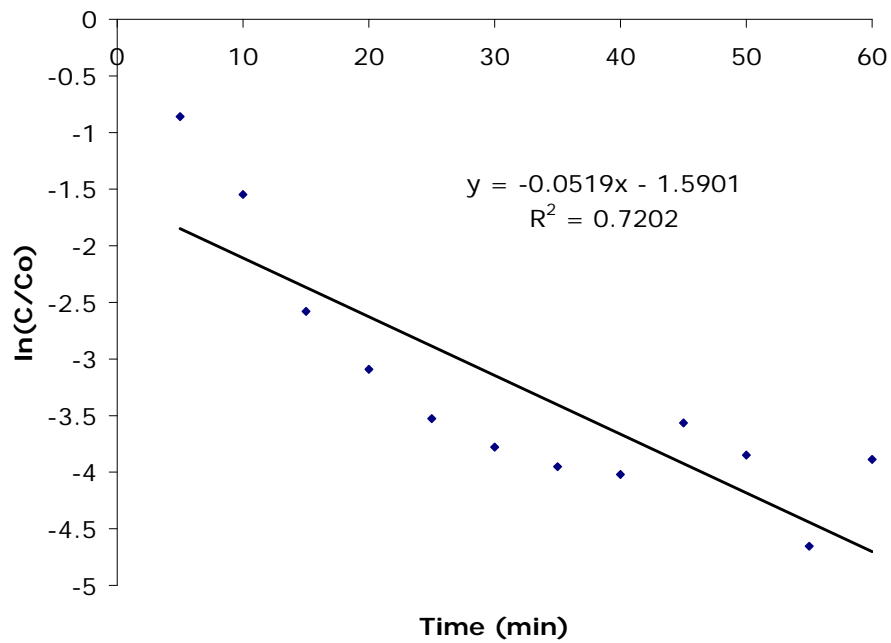
A7: First order kinetics MB Batch degradation 200g loading.



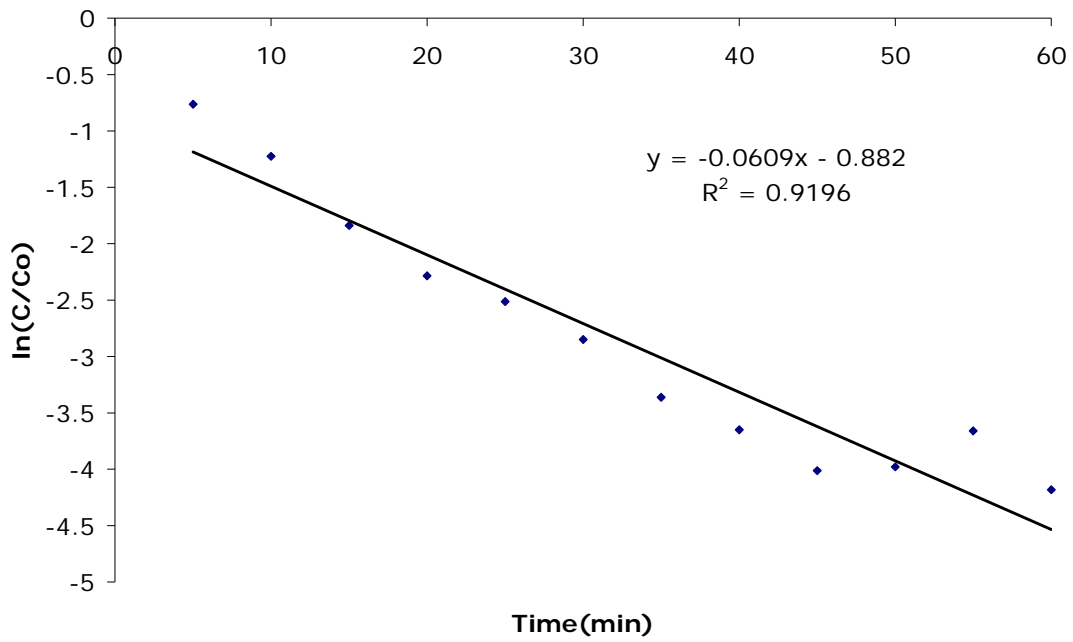
A8: First order kinetics MB Batch degradation 180g loading.



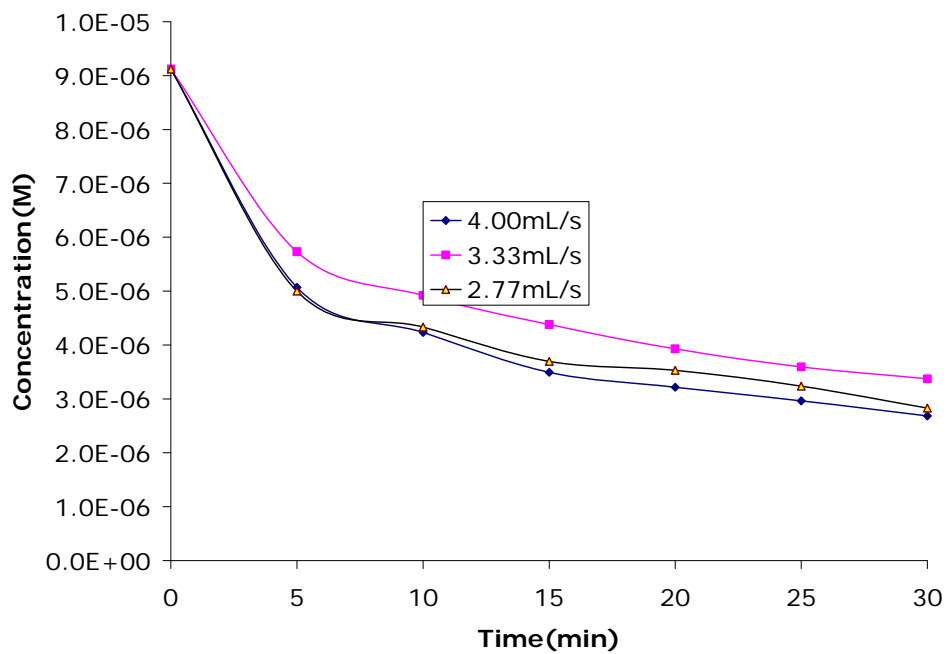
A9: First order kinetics MB Batch degradation 150g loading



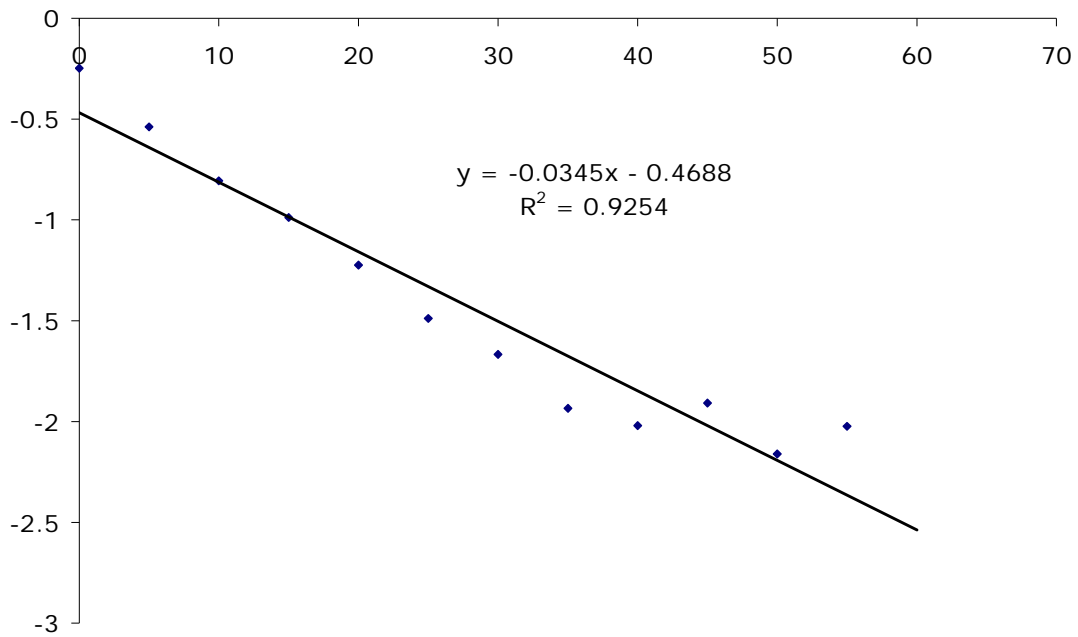
A10: First order kinetics MB Batch degradation 120g loading



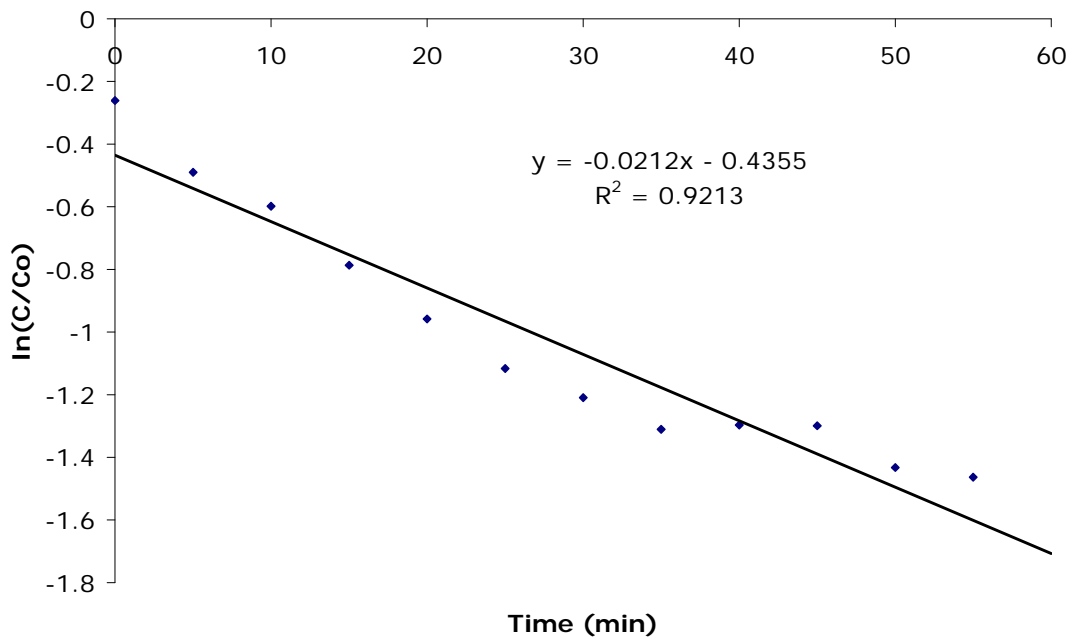
A11: First order kinetics MB Batch degradation 90g loading.



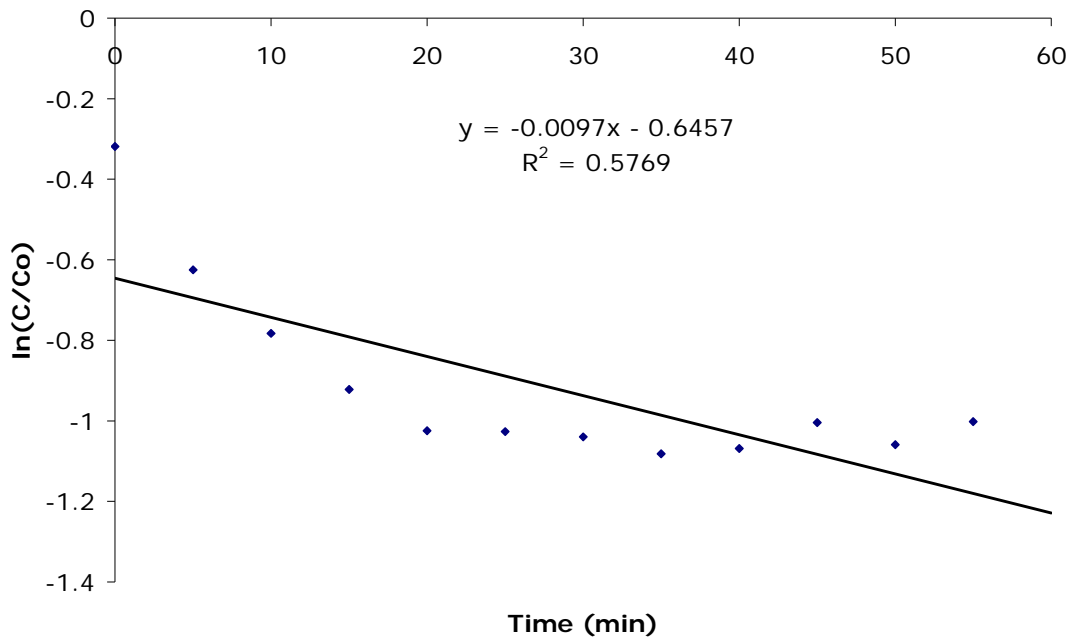
A12: Effect of recirculation rate on MB Adsorption. $C_0 = 10\mu\text{M}$, $\text{TiO}_2 = 30\text{ g}$.



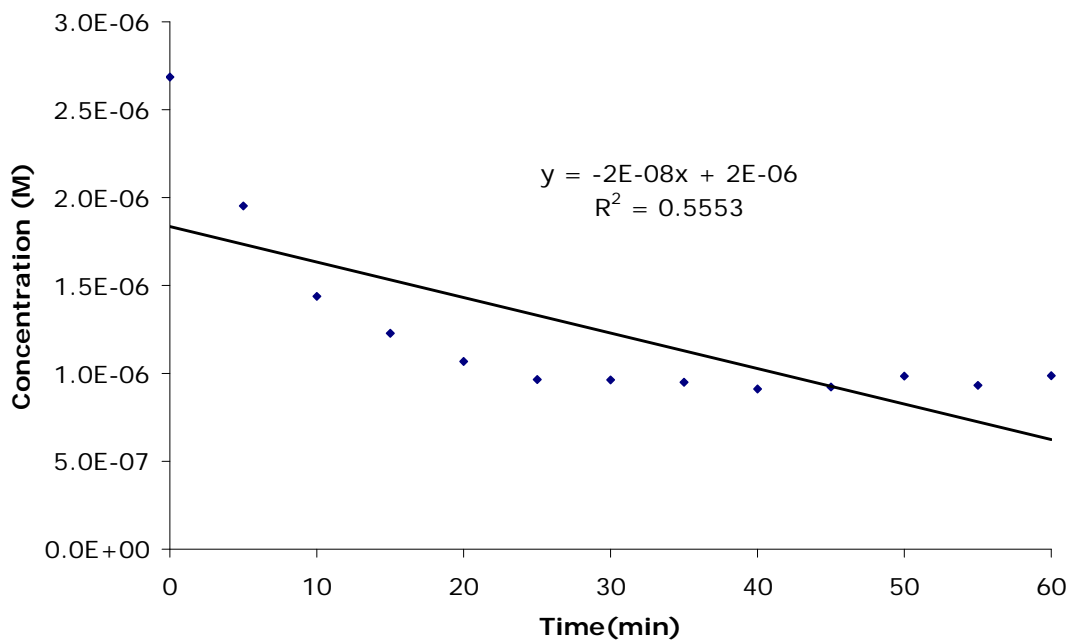
A13: Effect of recirculation rate on MB Adsorption. 2.77 mL/s (first order kinetics)



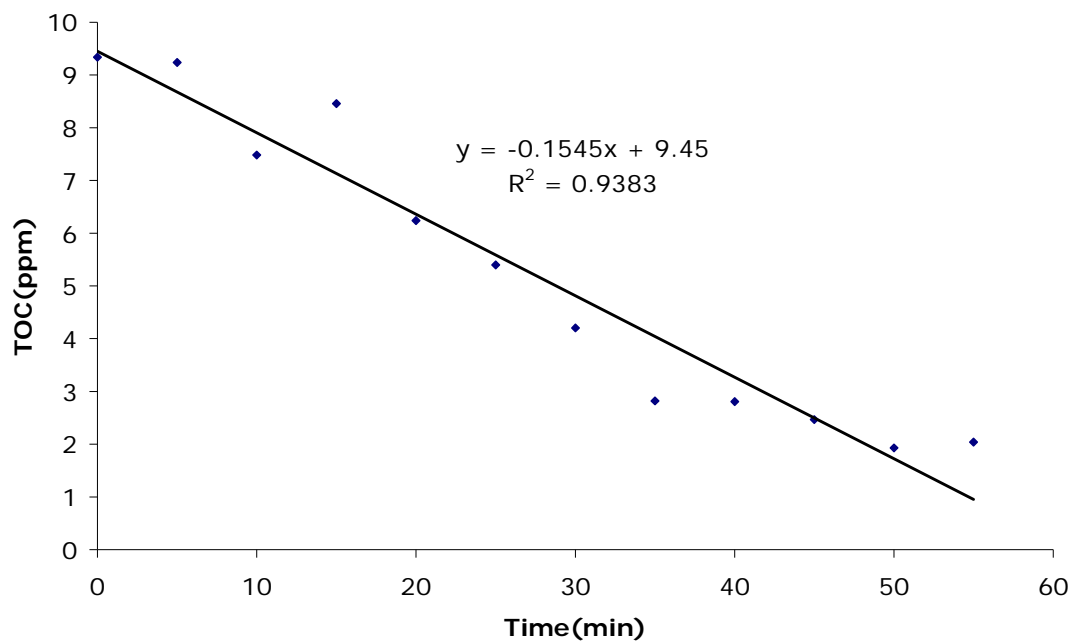
A14: Effect of recirculation rate on MB Adsorption. 3.33 mL/s (first order kinetics)



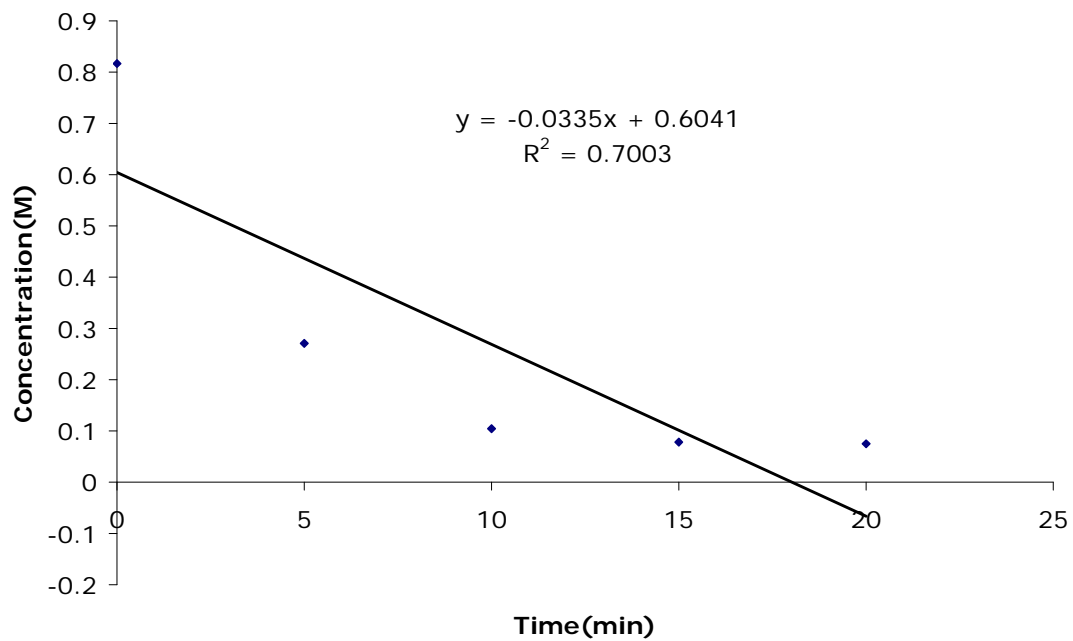
A15: Effect of recirculation rate on MB Adsorption. 4.00 mL/s (first order kinetic)



A16: Effect of recirculation rate on MB Adsorption. 4.00 mL/s (Zero order kinetics)



A17: Zero-order reaction kinetics of Produced Water mineralization on 30 g TiO₂ loading.



A18: P-25 MB degradation Zero-order reaction kinetics.